

Chapter 10. Radiation by Relativistic Charges

The discussion of special relativity in the previous chapter enables us to revisit the analysis of electromagnetic radiation by charged particles, now for arbitrary velocities. For a single point particle, it turns out to be possible to calculate the radiated wave fields in an explicit form and analyze the results for such important particular cases as synchrotron radiation and the “Bremsstrahlung” (brake radiation). After that, we will discuss the apparently unrelated effect of the so-called Coulomb losses of energy by a particle moving in condensed matter, because this discussion will naturally lead us to such important phenomena as the Cherenkov radiation and the transitional radiation. At the end of the chapter, I will briefly review the effects of the back action of the emitted radiation on the emitting particle, whose analysis reveals some limitations of classical electrodynamics.

10.1. Liénard-Wiechert potentials

A convenient starting point for the discussion of radiation by relativistic charges is provided by Eqs. (8.17) for the retarded potentials. In free space, these formulas with the integration variable notation changed from \mathbf{r}' to \mathbf{r}'' for the clarity of what follows, are reduced to

$$\phi(\mathbf{r}, t) = \frac{1}{4\pi\epsilon_0} \int \frac{\rho(\mathbf{r}'', t - R/c)}{R} d^3r'', \quad \mathbf{A}(\mathbf{r}, t) = \frac{\mu_0}{4\pi} \int \frac{\mathbf{j}(\mathbf{r}'', t - R/c)}{R} d^3r'', \quad \text{with } \mathbf{R} \equiv \mathbf{r} - \mathbf{r}''. \quad (10.1a)$$

As a reminder, Eqs. (1a) were derived from the Maxwell equations without any restrictions, and are very natural for situations with continuous distributions of the electric charge and/or current. However, for a single charged particle, whose charge and current distributions may be described as

$$\rho(\mathbf{r}, t) = q\delta(\mathbf{r} - \mathbf{r}'), \quad \mathbf{j}(\mathbf{r}, t) = q\mathbf{u}\delta(\mathbf{r} - \mathbf{r}'), \quad \text{with } \mathbf{u} \equiv \dot{\mathbf{r}}', \quad (10.1b)$$

where $\mathbf{r}' = \mathbf{r}'(t)$ is the instantaneous position of the charge, it is more convenient to recast Eqs. (1a) into an explicit form that would not require integration in each particular case. Indeed, as Eqs. (1) show, the potentials at a given observation point $\{\mathbf{r}, t\}$ are contributed by only one specific point $\{\mathbf{r}'(t_{\text{ret}}), t_{\text{ret}}\}$ of the particle's 4D trajectory (called its *world line*), which satisfies the following condition:

$$t_{\text{ret}} \equiv t - \frac{R_{\text{ret}}}{c}, \quad (10.2)$$

where t_{ret} is called the *retarded time*, and R_{ret} is the length of the following distance vector

$$\mathbf{R}_{\text{ret}} \equiv \mathbf{r}(t) - \mathbf{r}'(t_{\text{ret}}) \quad (10.3)$$

– physically, the distance covered by the electromagnetic wave from its emission to observation.

The reduction of Eqs. (1a) to such a simpler form, however, requires some care. Their naïve integration over \mathbf{r}'' would yield the following apparent but wrong results:

$$\phi(\mathbf{r}, t) = \frac{1}{4\pi\epsilon_0} \frac{q}{R_{\text{ret}}}, \quad \text{i.e.} \quad \frac{\phi(\mathbf{r}, t)}{c} = \frac{\mu_0}{4\pi} \frac{qc}{R_{\text{ret}}}; \quad \mathbf{A}(\mathbf{r}, t) = \frac{\mu_0}{4\pi} \frac{q\mathbf{u}_{\text{ret}}}{R_{\text{ret}}}, \quad \text{(WRONG!)} \quad (10.4)$$

where \mathbf{u}_{ret} is the particle's velocity at the retarded point $\mathbf{r}'(t_{\text{ret}})$. Eqs. (4) is a good example of how the relativity theory (even the special one :-) cannot be taken too lightly. Indeed, the strings (9.84)-(9.85), formed from the apparent potentials (4), would not obey the Lorentz transform rule (9.91), because according to Eqs. (2)-(3), the distance R_{ret} also depends on the reference frame it is measured in.

In order to correct the error, we need, first of all, to discuss the conditions (2)-(3). Combining them by eliminating R_{ret} , we get the following equation for t_{ret} :

$$c(t - t_{\text{ret}}) = |\mathbf{r}(t) - \mathbf{r}'(t_{\text{ret}})|. \tag{10.5}$$

Retarded time

Figure 1 depicts the graphical solution of this self-consistency equation as the only¹ point of intersection of the light cone of the observation point (see Fig. 9.9 and its discussion) and the particle's world line.

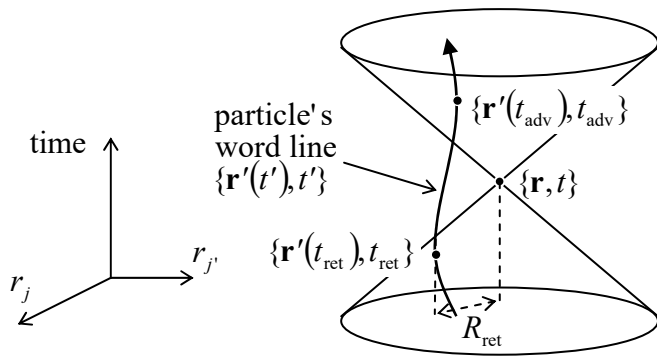


Fig. 10.1. Graphical solution of Eq. (5).

In Eq. (5), just as in Eqs. (1)-(3), all variables have to be measured in the inertial (“lab”) reference frame in which the observation point \mathbf{r} rests. Now let us write Eqs. (1) for a point charge in another inertial frame the frame $0'$ whose velocity (as measured in the lab frame) coincides, at the moment $t' = t_{\text{ret}}$, with the velocity \mathbf{u}_{ret} of the charge.² In that frame, the charge rests, so, as we know from the electro- and magnetostatics,

$$\phi' = \frac{q}{4\pi\epsilon_0 R'}, \quad \mathbf{A}' = 0. \tag{10.6a}$$

(Remember that this R' may not be equal to R_{ret} , because the latter distance is measured in the “lab” reference frame.) Let us use the identity $1/\epsilon_0 \equiv \mu_0 c^2$ again to rewrite Eqs. (6a) in the form of components of a 4-vector similar in structure to the last two of Eqs. (4):

$$\frac{\phi'}{c} = \frac{\mu_0 qc}{4\pi R'}, \quad \mathbf{A}' = 0. \tag{10.6b}$$

Now it is easy to guess the correct answer for the 4-potential for an arbitrary reference frame:

¹ As Fig. 1 shows, there is always another, “advanced” point $\{\mathbf{r}'(t_{\text{adv}}, t_{\text{adv}})\}$ of the particle's world line, with $t_{\text{adv}} > t$, which is also a solution of Eq. (5), but it does not fit Eqs. (1), because the observation, at the point $\{\mathbf{r}, t < t_{\text{adv}}\}$, of the field induced at the advanced point, would violate the causality principle.

² This is just a particular case of the *instantaneous reference frame* –the notion that was encountered in several exercise problems of the previous chapter, and indeed was implied (though admittedly not sufficiently advertised) as the derivation of the key Eq. (9.60).

$$A^\alpha = \frac{\mu_0}{4\pi} \frac{qc\mathbf{u}^\alpha}{u_\beta R^\beta}, \quad (10.7)$$

where (as a reminder) $A^\alpha \equiv \{\phi/c, \mathbf{A}\}$, $u^\alpha \equiv \gamma\{c, \mathbf{u}\}$, and R^α is the 4-vector of the inter-event distance, formed similarly to that of a single event – cf. Eq. (9.48):

$$R^\alpha \equiv \{c(t-t'), \mathbf{R}'\} \equiv \{c(t-t'), \mathbf{r}-\mathbf{r}'\}. \quad (10.8)$$

Indeed, we needed the 4-vector A^α that would:

- (i) obey the Lorentz transform,
- (ii) have its spatial components A_j scaling, at low velocity, as u_j , and
- (iii) be reduced to the correct result (6) in the instantaneous reference frame of the charge.

Eq. (7) evidently satisfies all these requirements, because the scalar product in its denominator is just

$$u_\beta R^\beta = \gamma\{c, -\mathbf{u}\} \cdot \{c(t-t'), \mathbf{R}'\} \equiv \gamma[c^2(t-t') - \mathbf{u} \cdot \mathbf{R}] = \gamma c(R - \boldsymbol{\beta} \cdot \mathbf{R}) \equiv \gamma cR(1 - \boldsymbol{\beta} \cdot \mathbf{n}), \quad (10.9)$$

where $\mathbf{n} \equiv \mathbf{R}/R$ is a unit vector in the observer's direction, $\boldsymbol{\beta} \equiv \mathbf{u}/c$ is the normalized velocity of the particle, and $\gamma \equiv 1/(1 - u^2/c^2)^{1/2}$. In the instantaneous reference frame of the charge (in which $\boldsymbol{\beta} = 0$ and $\gamma = 1$), the expression (9) is reduced to cR , so Eq. (7) is correctly reduced to Eq. (6b). Now let us spell out the components of Eq. (7) for the lab frame (in which $t' = t_{\text{ret}}$ and $R = R_{\text{ret}}$):

$$\phi(\mathbf{r}, t) = \frac{1}{4\pi\epsilon_0} \frac{q}{(R - \boldsymbol{\beta} \cdot \mathbf{R})_{\text{ret}}} \equiv \frac{1}{4\pi\epsilon_0} q \left[\frac{1}{R(1 - \boldsymbol{\beta} \cdot \mathbf{n})} \right]_{\text{ret}}, \quad (10.10a)$$

$$\mathbf{A}(\mathbf{r}, t) = \frac{\mu_0}{4\pi} q \left(\frac{\mathbf{u}}{R - \boldsymbol{\beta} \cdot \mathbf{R}} \right)_{\text{ret}} \equiv \frac{\mu_0}{4\pi} qc \left[\frac{\boldsymbol{\beta}}{R(1 - \boldsymbol{\beta} \cdot \mathbf{n})} \right]_{\text{ret}} \equiv \phi(\mathbf{r}, t) \frac{\mathbf{u}_{\text{ret}}}{c^2}. \quad (10.10b)$$

Liénard-
Wiechert
potentials

These formulas are called the *Liénard-Wiechert potentials*.³ In the non-relativistic limit, they coincide with the naïve guess (4), but in the general case include the additional factor $1/(1 - \boldsymbol{\beta} \cdot \mathbf{n})_{\text{ret}}$. Its physical origin may be illuminated by one more formal calculation – whose result we will need anyway. Let us differentiate the geometric relation (5), rewritten as

$$R_{\text{ret}} = c(t - t_{\text{ret}}), \quad (10.11)$$

over t_{ret} and then, independently, over t , assuming that \mathbf{r} is fixed. For that, let us first differentiate, over t_{ret} , both sides of the identity $R_{\text{ret}}^2 = \mathbf{R}_{\text{ret}} \cdot \mathbf{R}_{\text{ret}}$:

$$2R_{\text{ret}} \frac{\partial R_{\text{ret}}}{\partial t_{\text{ret}}} = 2\mathbf{R}_{\text{ret}} \cdot \frac{\partial \mathbf{R}_{\text{ret}}}{\partial t_{\text{ret}}}. \quad (10.12)$$

If \mathbf{r} is fixed, then $\partial \mathbf{R}_{\text{ret}} / \partial t_{\text{ret}} \equiv \partial(\mathbf{r} - \mathbf{r}') / \partial t_{\text{ret}} = -\partial \mathbf{r}' / \partial t_{\text{ret}} \equiv -\mathbf{u}_{\text{ret}}$, and Eq. (12) yields

$$\frac{\partial R_{\text{ret}}}{\partial t_{\text{ret}}} = \frac{\mathbf{R}_{\text{ret}}}{R_{\text{ret}}} \cdot \frac{\partial \mathbf{R}_{\text{ret}}}{\partial t_{\text{ret}}} = -(\mathbf{n} \cdot \mathbf{u})_{\text{ret}}. \quad (10.13)$$

Now let us differentiate the same R_{ret} over t . On one hand, Eq. (11) yields

³ They were derived in 1898 by Alfred-Marie Liénard and (independently) in 1900 by Emil Wiechert.

$$\frac{\partial R_{\text{ret}}}{\partial t} = c - c \frac{\partial t_{\text{ret}}}{\partial t}. \quad (10.14)$$

On the other hand, according to Eq. (5), at the partial differentiation over time, i.e. if \mathbf{r} is fixed, t_{ret} is a function of t alone, so (using Eq. (13) at the second step), we may write

$$\frac{\partial R_{\text{ret}}}{\partial t_{\text{ret}}} = \frac{\partial R_{\text{ret}}}{\partial t_{\text{ret}}} \frac{\partial t_{\text{ret}}}{\partial t} = -(\mathbf{n} \cdot \mathbf{u})_{\text{ret}} \frac{\partial t_{\text{ret}}}{\partial t}. \quad (10.15)$$

Now requiring Eqs. (14) and (15) to give the same result, we get:⁴

$$\frac{\partial t_{\text{ret}}}{\partial t} = \frac{c}{c - (\mathbf{n} \cdot \mathbf{u})_{\text{ret}}} \equiv \left(\frac{1}{1 - \boldsymbol{\beta} \cdot \mathbf{n}} \right)_{\text{ret}}. \quad (10.16) \quad \partial t_{\text{ret}} / \partial t$$

This important relation may be readily re-derived (and more clearly understood) for the particular case when the charge's velocity is directed straight toward the observation point. In this case, its vector \mathbf{u} resides in the same space-time plane as the observation point's world line $\mathbf{r} = \text{const}$ – say, the plane $[x, t]$ shown in Fig. 2.

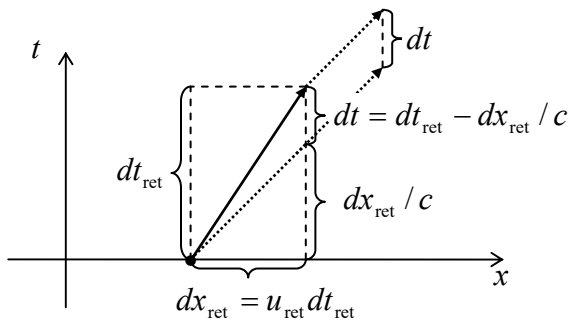


Fig. 10.2. Deriving Eq. (16) for the case $\boldsymbol{\beta} \cdot \mathbf{n} = \beta$.

Let us consider an elementary time interval $dt_{\text{ret}} \equiv dt'$, during which the particle would travel the space interval $dx_{\text{ret}} = u_{\text{ret}} dt_{\text{ret}}$. In Fig. 2, the corresponding segment of its world line is shown with a solid vector. The dotted vectors in this figure show the world lines of the radiation emitted by the particle in the beginning and at the end of this interval, and propagating with the speed of light c . As it follows from the drawing, the time interval dt between the instants of the arrival of the radiation from these two points to any time-independent spatial point of observation is

$$dt = dt_{\text{ret}} - \frac{dx_{\text{ret}}}{c} = dt_{\text{ret}} - \frac{u_{\text{ret}}}{c} dt_{\text{ret}}, \quad \text{so that} \quad \frac{dt_{\text{ret}}}{dt} = \frac{1}{1 - u_{\text{ret}}/c} \equiv \frac{1}{1 - \beta_{\text{ret}}}. \quad (10.17)$$

This expression coincides with Eq. (16) for our particular case when the directions of the vectors $\boldsymbol{\beta} \equiv \mathbf{u}/c$ and $\mathbf{n} \equiv \mathbf{R}/R$ (both taken at time t_{ret}) coincide, and hence $(\boldsymbol{\beta} \cdot \mathbf{n})_{\text{ret}} = \beta_{\text{ret}}$. The difference between Eqs. (16) and (17) may be interpreted by saying that the particle's velocity in the transverse directions (normal to the vector \mathbf{n}) is not important for this kinematic effect⁵ – the fact almost evident from Fig. 1.

⁴ This relation may be used for an alternative derivation of Eqs. (10) directly from Eqs (1) – the calculation left for the reader's exercise.

⁵ Note that this effect (linear in β) has nothing to do with the Lorentz time dilation (9.21), which is quadratic in β . (Indeed, all our arguments above referred to the same, lab frame.) Rather, it is close in nature to the Doppler effect.

So, the additional factor in the Liénard-Wiechert potentials is just the derivative $\partial t_{\text{ret}}/\partial t$. The reason for its appearance in Eqs. (10) is usually interpreted along the following lines. Let the charge q be spread along the direction of the vector \mathbf{R}_{ret} (in Fig. 2, along the x -axis) by an infinitesimal speed-independent interval δx_{ret} , so the linear density λ of its charge is proportional to $1/\delta x_{\text{ret}}$. Then the time rate of *charge's* arrival at some spatial point is $\lambda u_{\text{ret}} = \lambda \delta x_{\text{ret}}/dt_{\text{ret}}$, i.e. scales as $1/dt_{\text{ret}}$. However, the rate of *radiation's* arrival at the observation point scales as $1/dt$, so due to the non-zero velocity \mathbf{u}_{ret} of the particle, this rate differs from the charge arrival rate by the factor of dt_{ret}/dt , given by Eq. (16). (If the particle moves toward the observation point, $(\boldsymbol{\beta} \cdot \mathbf{n})_{\text{ret}} > 0$, as shown in Fig. 2, this factor is larger than 1.) This radiation compression effect leads to the field change (at $(\boldsymbol{\beta} \cdot \mathbf{n})_{\text{ret}} > 0$, its enhancement) by the same factor (16) – as described by Eqs. (10).

So, the 4-vector formalism was very instrumental for the calculation of field potentials. It may be also used to calculate the fields \mathbf{E} and \mathbf{B} – by plugging Eq. (7) into Eq. (9.124) to calculate the field strength tensor. This calculation yields

$$F^{\alpha\beta} = \frac{\mu_0 q}{4\pi} \frac{1}{u_\gamma R^\gamma} \frac{d}{d\tau} \left[\frac{R^\alpha u^\beta - R^\beta u^\alpha}{u_\delta R^\delta} \right]. \quad (10.18)$$

Now using Eq. (9.125) to identify the elements of this tensor with the field components, we may bring the result to the following vector form:⁶

$$\mathbf{E} = \frac{q}{4\pi\epsilon_0} \left[\frac{\mathbf{n} - \boldsymbol{\beta}}{\gamma^2 (1 - \boldsymbol{\beta} \cdot \mathbf{n})^3 R^2} + \frac{\mathbf{n} \times \{(\mathbf{n} - \boldsymbol{\beta}) \times \dot{\boldsymbol{\beta}}\}}{(1 - \boldsymbol{\beta} \cdot \mathbf{n})^3 cR} \right]_{\text{ret}}, \quad (10.19)$$

$$\mathbf{B} = \frac{\mathbf{n}_{\text{ret}} \times \mathbf{E}}{c}, \quad \text{i.e. } \mathbf{H} = \frac{\mathbf{n}_{\text{ret}} \times \mathbf{E}}{Z_0}. \quad (10.20)$$

Thus the magnetic and electric fields of a relativistic particle are always proportional and perpendicular to each other, and related just as in a plane wave – cf. Eq. (7.6), with the difference that now the vector \mathbf{n}_{ret} may be a function of time. Superficially, this result contradicts the electro- and magnetostatics, because, for a particle at rest, \mathbf{B} should vanish while \mathbf{E} stays finite. However, note that according to the Coulomb law for a point charge, in this case, $\mathbf{E} = E\mathbf{n}_{\text{ret}}$, so $\mathbf{B} \propto \mathbf{n}_{\text{ret}} \times \mathbf{E} \propto \mathbf{n}_{\text{ret}} \times \mathbf{n}_{\text{ret}} = 0$. (Actually, in these relations, the subscript “ret” is unnecessary.)

As a sanity check, let us use Eq. (19) as an alternative way to find the electric field of a charge moving without acceleration, i.e. uniformly, along a straight line – see Fig. 9.11a reproduced, with minor changes, in Fig. 3. (This calculation will also illustrate the technical challenges of practical applications of the Liénard-Wiechert formulas for even simple cases.) In this case, the vector $\boldsymbol{\beta}$ does not change in time, so the second term in Eq. (19) vanishes, and all we need to do is to spell out the Cartesian components of the first term.

⁶ An alternative way of deriving these formulas (highly recommended to the reader as an exercise) is to plug Eqs. (10) into the general relations (9.121), and carry out the required temporal and spatial differentiations directly, using Eq. (16) and its spatial counterpart (which may be derived absolutely similarly):

$$\nabla t_{\text{ret}} = - \left[\frac{\mathbf{n}}{c(1 - \boldsymbol{\beta} \cdot \mathbf{n})} \right]_{\text{ret}}.$$

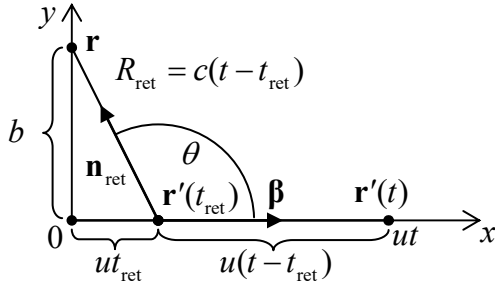


Fig. 10.3. The linearly moving charge problem.

Let us select the coordinate axes and the time origin as shown in Fig. 3, and make a clear distinction between the actual position, $\mathbf{r}'(t) = \{ut, 0, 0\}$ of the charged particle at the instant t we are considering, and its position $\mathbf{r}'(t_{\text{ret}})$ at the retarded instant defined by Eq. (5), i.e. the moment when the particle's field had to be radiated to reach the observation point \mathbf{r} at the given time t , propagating with the speed of light. In these coordinates

$$\boldsymbol{\beta} = \{\beta, 0, 0\}, \quad \mathbf{r} = \{0, b, 0\}, \quad \mathbf{r}'(t_{\text{ret}}) = \{ut_{\text{ret}}, 0, 0\}, \quad \mathbf{n}_{\text{ret}} = \{\cos \theta, \sin \theta, 0\}, \quad (10.21)$$

with $\cos \theta = -ut_{\text{ret}}/R_{\text{ret}}$, so $[(\mathbf{n} - \boldsymbol{\beta})_x]_{\text{ret}} = -ut_{\text{ret}}/R_{\text{ret}} - \beta$, and Eq. (19) yields, in particular:

$$E_x = \frac{q}{4\pi\epsilon_0} \frac{-ut_{\text{ret}}/R_{\text{ret}} - \beta}{\gamma^2 [(1 - \boldsymbol{\beta} \cdot \mathbf{n})^3 R^2]_{\text{ret}}} \equiv \frac{q}{4\pi\epsilon_0} \frac{-ut_{\text{ret}} - \beta R_{\text{ret}}}{\gamma^2 [(1 - \boldsymbol{\beta} \cdot \mathbf{n})^3 R^3]_{\text{ret}}}. \quad (10.22)$$

But according to Eq. (5), the product βR_{ret} may be represented as $\beta c(t - t_{\text{ret}}) \equiv u(t - t_{\text{ret}})$. Plugging this expression into Eq. (22), we may eliminate the explicit dependence of E_x on time t_{ret} :

$$E_x = \frac{q}{4\pi\epsilon_0} \frac{-ut}{\gamma^2 [(1 - \boldsymbol{\beta} \cdot \mathbf{n})R]_{\text{ret}}^3}. \quad (10.23)$$

The only non-zero transverse component of the field also has a similar form:

$$E_y = \frac{q}{4\pi\epsilon_0} \left[\frac{\sin \theta}{\gamma^2 (1 - \boldsymbol{\beta} \cdot \mathbf{n})^3 R^2} \right]_{\text{ret}} = \frac{q}{4\pi\epsilon_0} \frac{b}{\gamma^2 [(1 - \boldsymbol{\beta} \cdot \mathbf{n})R]_{\text{ret}}^3}, \quad (10.24)$$

while $E_z = 0$. From Fig. 3, $\boldsymbol{\beta} - \mathbf{n}_{\text{ret}} = \beta \cos \theta = -\beta ut_{\text{ret}}/R_{\text{ret}}$, so $(1 - \boldsymbol{\beta} \cdot \mathbf{n})R_{\text{ret}} \equiv R_{\text{ret}} + \beta ut_{\text{ret}}$, and we may again use Eq. (5) to get $(1 - \boldsymbol{\beta} \cdot \mathbf{n})R_{\text{ret}} = c(t - t_{\text{ret}}) + \beta ut_{\text{ret}} \equiv ct - ct_{\text{ret}}/\gamma^2$. What remains is to calculate t_{ret} from the self-consistency equation (5), whose square in our current case (Fig. 3) takes the form

$$R_{\text{ret}}^2 \equiv b^2 + (ut_{\text{ret}})^2 = c^2(t - t_{\text{ret}})^2. \quad (10.25)$$

This is a simple quadratic equation for t_{ret} , which (with the appropriate negative sign before the square root, to get $t_{\text{ret}} < t$) yields:

$$t_{\text{ret}} = \gamma^2 t - \left[(\gamma^2 t)^2 - \gamma^2 (t^2 - b^2/c^2) \right]^{1/2} \equiv \gamma^2 t - \frac{\gamma}{c} (u^2 \gamma^2 t^2 + b^2)^{1/2}, \quad (10.26)$$

so the only retarded-function combination that participates in Eqs. (23)-(24) is

$$[(1 - \boldsymbol{\beta} \cdot \mathbf{n})R]_{\text{ret}} = \frac{c}{\gamma^2} (u^2 \gamma^2 t^2 + b^2)^{1/2}, \quad (10.27)$$

and, finally, the electric field components are

$$E_x = -\frac{q}{4\pi\epsilon_0} \frac{\gamma u t}{(b^2 + \gamma^2 u^2 t^2)^{3/2}}, \quad E_y = \frac{q}{4\pi\epsilon_0} \frac{\gamma b}{(b^2 + \gamma^2 u^2 t^2)^{3/2}}, \quad E_z = 0. \quad (10.28)$$

But these are exactly Eqs. (9.139),⁷ which had been obtained in Sec. 9.5 by much simpler means, without the necessity to solve the self-consistency equation (5). However, that alternative approach was essentially based on the inertial motion of the particle, and cannot be used in problems in which it moves with acceleration. In such problems, the second term in Eq. (19), dropping with distance more slowly, as $1/R_{\text{ret}}$, and hence describing wave radiation, is frequently the most important one.

10.2. Radiation power

Let us calculate the angular distribution of the particle's radiation. For that, we need to return to Eqs. (19)-(20) to find the Poynting vector $\mathbf{S} = \mathbf{E} \times \mathbf{H}$, and in particular, its radial component $S_n = \mathbf{S} \cdot \mathbf{n}_{\text{ret}}$, at large distances R from the particle. Following tradition,⁸ let us express the result as the energy radiated into unit solid angle per unit time interval dt_{rad} of the *radiation*, rather than that (dt) of its *measurement*. (We will need to return to the measurement time t in the next section to calculate the observed radiation spectrum.) Using Eq. (16), we get

$$\frac{d\mathcal{P}}{d\Omega} \equiv -\frac{d\mathcal{E}}{d\Omega dt_{\text{ret}}} = (R^2 S_n)_{\text{ret}} \frac{\partial t}{\partial t_{\text{ret}}} = (\mathbf{E} \times \mathbf{H}) \cdot [R^2 \mathbf{n} (1 - \boldsymbol{\beta} \cdot \mathbf{n})]_{\text{ret}}. \quad (10.29)$$

At sufficiently large distances from the particle, i.e. in the limit $R_{\text{ret}} \rightarrow \infty$ (in the *radiation zone*), the contribution of the first (essentially, the Coulomb-field) term in the square brackets of Eq. (19) vanishes as $1/R^2$, and the substitution of the remaining term into Eqs. (20) and then Eq. (29) yields the following formula, which is valid for an arbitrary law of the particle's motion:⁹

Radiation
power
density

$$\frac{d\mathcal{P}}{d\Omega} = \frac{Z_0 q^2}{(4\pi)^2} \frac{|\mathbf{n} \times [(\mathbf{n} - \boldsymbol{\beta}) \times \dot{\boldsymbol{\beta}}]|^2}{(1 - \mathbf{n} \cdot \boldsymbol{\beta})^5}. \quad (10.30)$$

Now, let us apply this important result to some simple cases. First of all, Eq. (30) says that a charge moving with a constant velocity $\boldsymbol{\beta}$ does not radiate at all. This might be expected from our analysis of this case in Sec. 9.5 because in the reference frame moving with the charge it produces only the Coulomb electrostatic field, i.e. no radiation.

Next, let us consider a linear motion of a point charge with a non-zero acceleration directed along the straight line of the motion. In this case, with the coordinate axes selected as shown in Fig. 4a, each of the vectors involved in Eq. (30) has at most two non-zero Cartesian components:

⁷ A similar calculation of magnetic field components from Eq. (20) gives results identical to Eqs. (9.140).

⁸ This tradition may be reasonably justified. Indeed, we may say that the radiation field “detaches” from the particle at times close to t_{ret} , while the observation time t depends on the detector's position, and hence is less relevant for the radiation process as such.

⁹ If the direction of radiation, \mathbf{n} , does not change in time, this formula does not depend on the observer's position \mathbf{R} . Hence, from this point on, the index “ret” may be safely dropped for brevity, though we should always remember that $\boldsymbol{\beta}$ in Eq. (30) is the reduced velocity of the particle at the instant of the radiation's *emission*, not of its observation.

$$\mathbf{n} = \{\sin \theta, 0, \cos \theta\}, \quad \boldsymbol{\beta} = \{0, 0, \beta\}, \quad \dot{\boldsymbol{\beta}} = \{0, 0, \dot{\beta}\}, \quad (10.31)$$

where θ is the angle between the directions of the particle's motion and of the radiation's propagation. Plugging these expressions into Eq. (30) and performing the vector multiplications, we readily get

$$\frac{d\mathcal{P}}{d\Omega} = \frac{Z_0 q^2}{(4\pi)^2} \dot{\beta}^2 \frac{\sin^2 \theta}{(1 - \beta \cos \theta)^5}. \quad (10.32)$$

Figure 4b shows the angular distribution of such radiation, for three values of the particle's speed u .

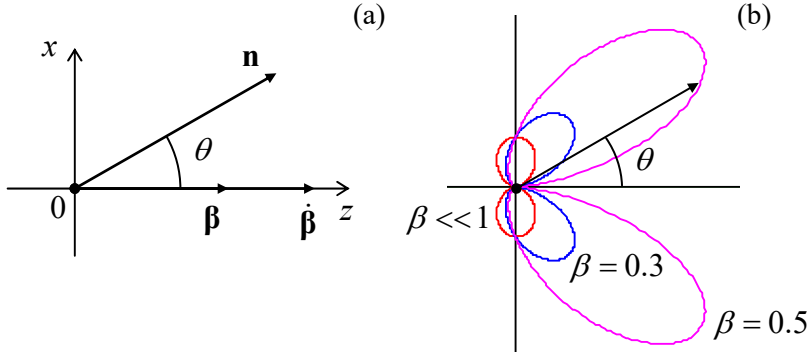


Fig. 10.4. Particle's radiation at its linear acceleration: (a) the problem's geometry, and (b) the last fraction of Eq. (32) as a function of the angle θ .

If the speed is relatively low ($u \ll c$, i.e. $\beta \ll 1$), the denominator in Eq. (32) is very close to 1 for all observation angles θ , so the angular distribution of the radiation power is close to $\sin^2 \theta$ – just as it follows from the general non-relativistic Larmor formula (8.26), for our current case with $\Theta = \theta$. However, as the velocity is increased, the denominator becomes less than 1 for $\theta < \pi/2$, i.e. for the forward-looking directions, and larger than 1 for back directions. As a result, the radiation in the direction of the particle's motion is increased (somewhat counter-intuitively, regardless of the acceleration's sign!), while that in the back direction is suppressed. For ultra-relativistic particles ($\beta \rightarrow 1$), this trend is strongly exacerbated, and radiation to very small forward angles dominates. To describe this main part of the angular distribution, we may expand the trigonometric functions of θ participating in Eq. (32) in the Taylor series in small θ , and keep only their leading terms: $\sin \theta \approx \theta$, $\cos \theta \approx 1 - \theta^2/2$, so $(1 - \beta \cos \theta) \approx (1 + \gamma^2 \theta^2)/2\gamma^2$. The resulting expression,

$$\frac{d\mathcal{P}}{d\Omega} \approx \frac{2Z_0 q^2}{\pi^2} \dot{\beta}^2 \gamma^8 \frac{(\gamma \theta)^2}{(1 + \gamma^2 \theta^2)^5}, \quad \text{for } \gamma \gg 1, \quad (10.33)$$

describes a narrow “hollow cone” distribution of radiation, with its maximum at the angle

$$\theta_0 = \frac{1}{2\gamma} \ll 1. \quad (10.34)$$

Another important aspect of Eq. (33) is how extremely fast (as γ^8) the radiation density grows with the Lorentz factor γ , i.e. with the particle's energy $\mathcal{E} = \gamma mc^2$.

Still, the total radiated power \mathcal{P} (into all observation angles) at linear acceleration is not too high for any practicable values of parameters. To show this, let us first calculate \mathcal{P} for an arbitrary motion of the particle. To start, let me demonstrate how \mathcal{P} may be found (or rather guessed) from the general relativistic arguments. In Sec. 8.2, we have derived Eq. (8.27) for the power of the electric dipole radiation for a non-relativistic particle motion. That result is valid, in particular, for one charged particle,

whose electric dipole moment's derivative over time may be expressed as $d(q\mathbf{r})/dt = (q/m)\mathbf{p}$, where \mathbf{p} is the particle's linear mechanical momentum (*not* its electric dipole moment). As a result, the Larmor formula (8.27) in free space, i.e. with $v = c$ (but $u \ll c$) reduces to

$$\mathcal{P} = \frac{Z_0}{6\pi c^2} \left(\frac{q}{m} \frac{d\mathbf{p}}{dt} \right)^2 \equiv \frac{Z_0 q^2}{6\pi m^2 c^2} \left(\frac{d\mathbf{p}}{dt} \cdot \frac{d\mathbf{p}}{dt} \right), \quad \text{for } u \ll c. \quad (10.35)$$

This is evidently not a Lorentz-invariant result, but it gives a clear hint of how such an invariant, which would be reduced to Eq. (35) in the non-relativistic limit, may be formed:

$$\mathcal{P} = -\frac{Z_0 q^2}{6\pi m^2 c^2} \left(\frac{dp_\alpha}{d\tau} \cdot \frac{dp^\alpha}{d\tau} \right) \equiv \frac{Z_0 q^2}{6\pi m^2 c^2} \left[\left(\frac{d\mathbf{p}}{d\tau} \right)^2 - \frac{1}{c^2} \left(\frac{d\mathcal{E}}{d\tau} \right)^2 \right]. \quad (10.36)$$

Using the relativistic expressions $\mathbf{p} = \gamma mc\boldsymbol{\beta}$, $\mathcal{E} = \gamma mc^2$, and $d\tau = dt/\gamma$, the last formula may be recast into the so-called *Liénard extension* of the Larmor formula:¹⁰

$$\mathcal{P} = \frac{Z_0 q^2}{6\pi} \gamma^6 \left[(\dot{\boldsymbol{\beta}})^2 - (\boldsymbol{\beta} \times \dot{\boldsymbol{\beta}})^2 \right] \equiv \frac{Z_0 q^2}{6\pi} \gamma^4 \left[(\dot{\boldsymbol{\beta}})^2 + \gamma^2 (\boldsymbol{\beta} \cdot \dot{\boldsymbol{\beta}})^2 \right]. \quad (10.37)$$

Total
radiation
power via $\boldsymbol{\beta}$

It may be also obtained by direct integration of Eq. (30) over the full solid angle, thus confirming our guess.

However, for some applications, it is beneficial to express \mathcal{P} via the time evolution of the particle's momentum alone. For that, we may differentiate the fundamental relativistic relation (9.78), $\mathcal{E}^2 = (mc^2)^2 + (pc)^2$, over the proper time τ to get

$$2\mathcal{E} \frac{d\mathcal{E}}{d\tau} = 2c^2 p \frac{dp}{d\tau}, \quad \text{i.e.} \quad \frac{d\mathcal{E}}{d\tau} = \frac{c^2 p}{\mathcal{E}} \frac{dp}{d\tau} = u \frac{dp}{d\tau}, \quad (10.38)$$

where the last step used the relativistic relation $c^2 \mathbf{p}/\mathcal{E} = \mathbf{u}$ mentioned in Sec. 9.3. Plugging Eq. (38) into Eq. (36), we may rewrite it as

$$\mathcal{P} = \frac{Z_0 q^2}{6\pi m^2 c^2} \left[\left(\frac{d\mathbf{p}}{d\tau} \right)^2 - \beta^2 \left(\frac{dp}{d\tau} \right)^2 \right]. \quad (10.39)$$

Total
radiation
power via \mathbf{p}

Please note the difference between the squared derivatives in this expression: in the first of them we have to differentiate the momentum's vector \mathbf{p} first, and only then form a scalar by squaring the resulting vector derivative, while in the second case, only the magnitude of the vector has to be differentiated. For example, for circular motion with a constant speed (to be analyzed in detail in the next section), the second term vanishes, while the first one does not.

However, if we return to the simplest case of linear acceleration (Fig. 4), then $(d\mathbf{p}/d\tau)^2 = (dp/d\tau)^2$, and Eq. (39) is reduced to

¹⁰ The second form of Eq. (10.37), which is frequently more convenient for applications, may be readily obtained from the first one by applying MA Eq. (7.7a) to the vector product.

$$\mathcal{P} = \frac{Z_0 q^2}{6\pi m^2 c^2} \left(\frac{dp}{d\tau} \right)^2 (1 - \beta^2) \equiv \frac{Z_0 q^2}{6\pi m^2 c^2} \left(\frac{dp}{d\tau} \right)^2 \frac{1}{\gamma^2} \equiv \frac{Z_0 q^2}{6\pi m^2 c^2} \left(\frac{dp}{dt_{\text{ret}}} \right)^2, \quad (10.40)$$

i.e. formally coincides with the non-relativistic relation (35). To get a better feeling of the magnitude of this radiation, we may combine Eq. (9.144) with $\mathbf{B} = 0$, and Eq. (9.148) with $\mathbf{E} \parallel \mathbf{u}$ to get $dp/dt_{\text{ret}} = d\mathcal{E}/dz'$, where z' is the particle's coordinate at the moment t_{ret} . The last relation allows us to rewrite Eq. (40) in the following form:

$$\mathcal{P} = \frac{Z_0 q^2}{6\pi m^2 c^2} \left(\frac{d\mathcal{E}}{dz} \right)^2 \equiv \frac{Z_0 q^2}{6\pi m^2 c^2} \frac{d\mathcal{E}}{dz'} \frac{d\mathcal{E}}{dt_{\text{ret}}} \frac{dt_{\text{ret}}}{dz'} \equiv \frac{Z_0 q^2}{6\pi m^2 c^2 u} \frac{d\mathcal{E}}{dz'} \frac{d\mathcal{E}}{dt_{\text{ret}}}. \quad (10.41)$$

For the most important case of ultra-relativistic motion ($u \rightarrow c$), this result reduces to

$$\frac{\mathcal{P}}{d\mathcal{E}/dt_{\text{ret}}} \approx \frac{2}{3} \frac{d(\mathcal{E}/mc^2)}{d(z'/r_c)}, \quad (10.42)$$

where r_c is the classical radius of the particle, defined by Eq. (8.41). This formula shows that the radiated power, i.e. the change of the particle's energy due to radiation, is much smaller than that due to the accelerating field unless energy as large as $\sim mc^2$ is gained on the classical radius of the particle. For example, for an electron, with $r_c \approx 3 \times 10^{-15}$ m and $mc^2 = m_e c^2 \approx 0.5$ MeV, such an acceleration would require the accelerating electric field of the order of $(0.5 \text{ MV})/(3 \times 10^{-15} \text{ m}) \sim 10^{14}$ MV/m, while practicable accelerating fields are below 10^2 MV/m – limited by the electric breakdown effects. (As described by the factor m^2 in the denominator of Eq. (41), for heavier particles such as protons, the relative losses are even lower.) Such negligible radiative losses of energy are actually a large advantage of linear accelerators – such as the famous two-mile-long SLAC,¹¹ which can accelerate electrons or positrons to energies up to 50 GeV, i.e. to $\gamma \approx 10^5$. If obtaining radiation from the accelerated particles is the goal, it may be readily achieved by bending their trajectories using additional magnetic fields – see the next section.

10.3. Synchrotron radiation

Now let us consider a charged particle being accelerated in the direction perpendicular to its velocity \mathbf{u} (for example by the magnetic component of the Lorentz force), so its speed u , and hence the magnitude p of its momentum, do not change. In this case, the second term in the square brackets of Eq. (39) vanishes, and it yields

$$\mathcal{P} = \frac{Z_0 q^2}{6\pi m^2 c^2} \left(\frac{d\mathbf{p}}{d\tau} \right)^2 = \frac{Z_0 q^2}{6\pi m^2 c^2} \left(\frac{d\mathbf{p}}{dt_{\text{ret}}} \right)^2 \gamma^2. \quad (10.43)$$

Comparing this expression with Eq. (40), we see that for the same acceleration magnitude, the electromagnetic radiation is a factor of γ^2 larger. For modern accelerators, with $\gamma \sim 10^4$ - 10^5 , such a factor creates an enormous difference. For example, if a particle is on a cyclotron orbit in a constant magnetic field (as was analyzed in Sec. 9.6), both \mathbf{u} and $\mathbf{p} = \gamma m \mathbf{u}$ obey Eq. (9.150), so

¹¹ See, e.g., <https://www6.slac.stanford.edu/>.

$$\left| \frac{d\mathbf{p}}{dt_{\text{ret}}} \right| = \omega_c p = \frac{u}{R} p = \beta^2 \gamma \frac{mc^2}{R}, \quad (10.44)$$

(where R is the orbit's radius), so for the power of this *synchrotron radiation*, Eq. (43) yields

$$\mathcal{P} = \frac{Z_0 q^2}{6\pi} \beta^4 \gamma^4 \frac{c^2}{R^2} \equiv \frac{1}{4\pi\epsilon_0} \frac{2}{3} \frac{q^4 B^2}{m^2 c} \beta^2 \gamma^2. \quad (10.45)$$

Synchrotron
radiation:
total power

Note that for ultrarelativistic particles ($\beta \approx 1$), the power grows as γ^2 , i.e. as the square of the particle's energy $\mathcal{E} \propto \gamma$. For example, for typical parameters of the first electron cyclotrons (such as the General Electric's machine in which the synchrotron radiation was first noticed in 1947), $R \sim 1$ m, $\mathcal{E} \sim 0.3$ GeV ($\gamma \sim 600$), Eq. (45) gives a very modest electron energy loss per one revolution: $\mathcal{P}\mathcal{T} \equiv \mathcal{A}(2\pi R/u) \approx 2\pi\mathcal{P}R/c \sim 1$ keV. However, already by the mid-1970s, electron accelerators, with $R \sim 100$ m, could give each particle energy $\mathcal{E} \sim 10$ GeV, and the energy loss per revolution grew to ~ 10 MeV, becoming the major energy loss mechanism. For proton accelerators, such energy loss is much less of a problem, because the γ of an ultra-relativistic particle (at fixed \mathcal{E}) is proportional to $1/m$, so the estimates, at the same R , should be scaled back by $(m_p/m_e)^4 \sim 10^{13}$. Nevertheless, in the giant modern accelerators such as the LHC (with $R \approx 4.3$ km and \mathcal{E} up to 7 TeV), the synchrotron radiation loss per revolution is rather noticeable ($\mathcal{P}\mathcal{T} \sim 6$ keV), leading not as much to particle deceleration as to a substantial photoelectron emission from the beam tube's walls, creating harmful defocusing effects.

However, what is bad for particle accelerators and storage rings is good for the so-called *synchrotron light sources* – the electron accelerators designed for the generation of intensive synchrotron radiation – with the spectrum extending well beyond the visible light range. Let us analyze the angular and spectral distributions of such radiation. To calculate the angular distribution, let us select the coordinate axes as shown in Fig. 5, with the origin at the current location of the orbiting particle, the z -axis directed along its instant velocity (i.e. the vector $\boldsymbol{\beta}$), and the x -axis, toward the orbit's center.

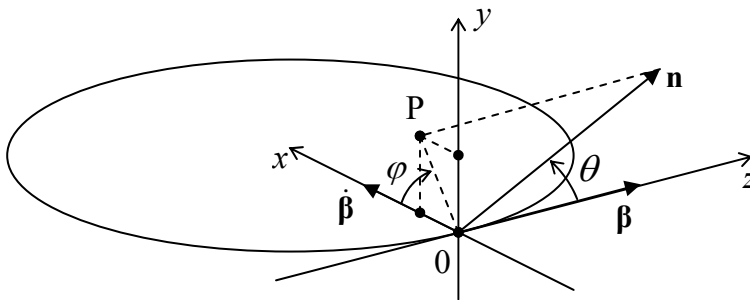


Fig. 10.5. The synchrotron radiation problem's geometry.

In the general case, when the unit vector \mathbf{n} toward the radiation's observer is not within any of the coordinate planes, it has to be described by two angles – the polar angle θ , and the azimuthal angle φ between the x -axis and the projection OP of the vector \mathbf{n} onto the $[x, y]$ -plane. Since the length of the segment OP is $\sin\theta$, the Cartesian components of the relevant vectors are as follows:

$$\mathbf{n} = \{\sin\theta \cos\varphi, \sin\theta \sin\varphi, \cos\theta\}, \quad \boldsymbol{\beta} = \{0, 0, \beta\}, \quad \text{and} \quad \dot{\boldsymbol{\beta}} = \{\dot{\beta}, 0, 0\}. \quad (10.46)$$

Plugging these expressions into the general Eq. (30), we get

$$\frac{d\mathcal{P}}{d\Omega} = \frac{2Z_0 q^2}{\pi^2} |\dot{\boldsymbol{\beta}}|^2 \gamma^6 f(\theta, \varphi), \quad \text{where} \quad (10.47)$$

$$f(\theta, \varphi) \equiv \frac{1}{8\gamma^6 (1 - \beta \cos \theta)^3} \left[1 - \frac{\sin^2 \theta \cos^2 \varphi}{\gamma^2 (1 - \beta \cos \theta)^2} \right],$$

Synchrotron
radiation:
angular
distribution

According to this result, just as at the linear acceleration, in the ultra-relativistic limit, most radiation goes into a narrow cone (of a width $\Delta\theta \sim \gamma^{-1} \ll 1$) around the vector $\boldsymbol{\beta}$, i.e. around the instant direction of the particle's propagation. For such small angles, and $\gamma \gg 1$,

$$f(\theta, \varphi) \approx \frac{1}{(1 + \gamma^2 \theta^2)^3} \left[1 - \frac{4\gamma^2 \theta^2 \cos^2 \varphi}{(1 + \gamma^2 \theta^2)^2} \right]. \quad (10.48)$$

The left panel of Fig. 6 shows a color-coded contour map of this angular distribution $f(\theta, \varphi)$, as observed on a distant plane normal to the particle's instant velocity (in Fig. 5, parallel to the $[x, y]$ -plane), while its right panel shows the factor f as a function of θ in two perpendicular directions: within the particle's rotation plane (in the direction parallel to the x -axis, i.e. at $\varphi = 0$) and perpendicular to this plane (along the y -axis, i.e. at $\varphi = \pm\pi/2$). The result shows, first of all, that, in contrast to the case of linear acceleration, the narrow radiation cone is now not hollow: the intensity maximum is reached at $\theta = 0$, i.e. exactly in the direction of the particle's motion direction. Second, the radiation cone is not axially symmetric: within the particle rotation plane, the intensity drops faster (and even has nodes at $\theta = \pm 1/\gamma$).

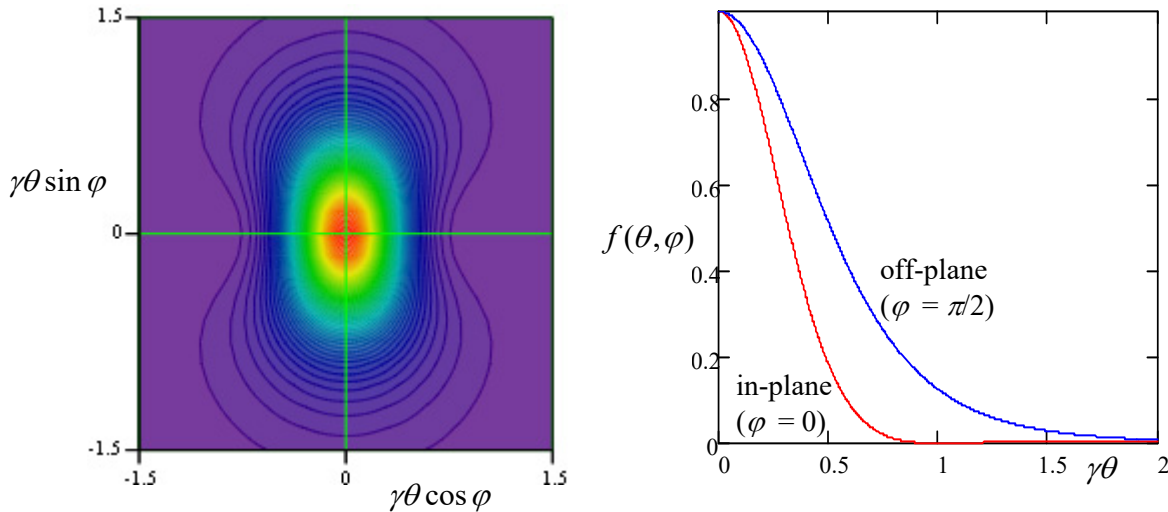


Fig. 10.6. The angular distribution of the synchrotron radiation at $\gamma \gg 1$.

The angular distribution (47) of the synchrotron radiation was calculated for the (inertial) reference frame whose origin coincides with the particle's position at this particular instant, i.e. its radiation pattern is time-independent in the frame moving with the particle. This pattern enables a semi-quantitative description of the radiation by an ultra-relativistic particle from the point of view of a stationary observer: if the observation point is on (or very close to) the rotation plane,¹² it is being

¹² It is easy (and hence is left for the reader's exercise) to show that if the observation point is much off-plane (say, is located on the particle orbit's axis), the radiation is virtually monochromatic, with frequency ω_c . (As we know from Sec. 8.2, in the non-relativistic limit $u \ll c$, this is true for *any* observation point.)

“struck” by the narrow radiation cone once each rotation period $\mathcal{T} \approx 2\pi R/c$, each “strike” giving a field pulse of a short duration $\Delta t_{\text{ret}} \ll 1/\omega_c$ – see Fig. 7.¹³

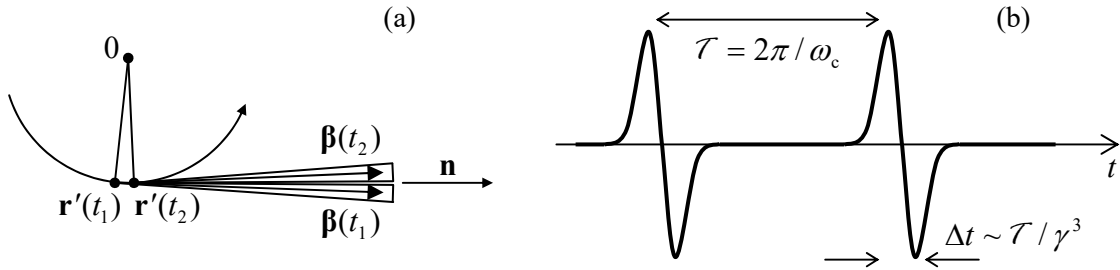


Fig. 10.7. (a) The synchrotron radiation cones (at $\gamma \gg 1$) for two close values of t_{ret} , and (b) the in-plane component of the electric field observed in the rotation plane, as a function of time t – schematically.

The evaluation of the time duration Δt of each pulse requires some care: its estimate $\Delta t_{\text{ret}} \sim 1/\gamma\omega_c$ is correct for the duration of the retarded time interval during which its cone is aimed at the observer. However, due to the time compression effect discussed in detail in Sec. 1 and described by Eq. (16), the pulse duration as seen by the observer is a factor of $1/(1 - \beta)$ shorter, so

$$\Delta t = (1 - \beta)\Delta t_{\text{ret}} \sim \frac{1 - \beta}{\gamma\omega_c} \sim \frac{1}{\gamma^3\omega_c} \sim \gamma^{-3}\mathcal{T}, \quad \text{for } \gamma \gg 1. \quad (10.49)$$

From the Fourier theorem, we can expect the frequency spectrum of such radiation to consist of numerous ($N \sim \gamma^3 \gg 1$) harmonics of the particle rotation frequency ω_c , with comparable amplitudes. However, if the orbital frequency fluctuates even slightly ($\delta\omega/\omega_c > 1/N \sim 1/\gamma^3$), as it happens in most practical systems, the radiation pulses are not coherent, so the average radiation power spectrum may be calculated as that of one pulse, multiplied by the number of pulses per second. In this case, the spectrum is continuous, extending from low frequencies all the way to approximately

$$\omega_{\text{max}} \sim 1/\Delta t \sim \gamma^3\omega_c. \quad (10.50)$$

In order to verify and quantify this result, let us calculate the spectrum of radiation due to a single pulse. For that, we should first make the general notion of the radiation spectrum quantitative. Let us represent an arbitrary electric field (say that of the synchrotron radiation we are studying now) observed at a fixed point \mathbf{r} , as a function of the *observation* time t , as a Fourier integral:¹⁴

$$\mathbf{E}(t) = \int_{-\infty}^{+\infty} \mathbf{E}_\omega e^{-i\omega t} dt. \quad (10.51)$$

¹³ The fact that the in-plane component of each electric field’s pulse $\mathbf{E}(t)$ is antisymmetric with respect to its central point, and hence vanishes at that point (as Fig. 7b shows), readily follows from Eq. (19).

¹⁴ In contrast to the single-frequency case (i.e. a monochromatic wave), we may avoid taking the real part of the complex function ($\mathbf{E}_\omega e^{-i\omega t}$) by requiring that in Eq. (51), $\mathbf{E}_{-\omega} = \mathbf{E}_\omega^*$. However, it is important to remember the factor $1/2$ required for the transition to a monochromatic wave of frequency ω_0 and with real amplitude \mathbf{E}_0 : $\mathbf{E}_\omega = \mathbf{E}_0 [\delta(\omega - \omega_0) + \delta(\omega + \omega_0)]/2$.

This expression may be plugged into the formula for the total energy of the radiation pulse (i.e. of the loss of particle's energy \mathcal{E}) per unit solid angle:¹⁵

$$-\frac{d\mathcal{E}}{d\Omega} \equiv \int_{-\infty}^{+\infty} S_n(t) R^2 dt = \frac{R^2}{Z_0} \int_{-\infty}^{+\infty} |\mathbf{E}(t)|^2 dt. \quad (10.52)$$

This substitution, followed by a natural change of the integration order, yields

$$-\frac{d\mathcal{E}}{d\Omega} = \frac{R^2}{Z_0} \int_{-\omega}^{+\omega} d\omega \int_{-\omega}^{+\omega} d\omega' \mathbf{E}_\omega \cdot \mathbf{E}_{\omega'} \int_{-\infty}^{+\infty} dt e^{-i(\omega+\omega')t}. \quad (10.53)$$

But the inner integral (over t) is just $2\pi\delta(\omega + \omega')$.¹⁶ This delta function kills one of the frequency integrals (say, one over ω'), and Eq. (53) gives us a result that may be recast as

$$-\frac{d\mathcal{E}}{d\Omega} = \int_0^{+\infty} I(\omega) d\omega, \quad \text{with } I(\omega) \equiv \frac{4\pi R^2}{Z_0} \mathbf{E}_\omega \cdot \mathbf{E}_{-\omega} \equiv \frac{4\pi R^2}{Z_0} \mathbf{E}_\omega \cdot \mathbf{E}_\omega^*, \quad (10.54)$$

where the evident frequency symmetry of the scalar product $\mathbf{E}_\omega \cdot \mathbf{E}_{-\omega}$ has been utilized to fold the integral of $I(\omega)$ to positive frequencies only. The first of Eqs. (54) makes the physical sense of the function $I(\omega)$ very clear: this is the so-called *spectral density* of the electromagnetic radiation (per unit solid angle).¹⁷

To calculate the spectral density, we can express the function \mathbf{E}_ω via $\mathbf{E}(t)$ using the Fourier transform reciprocal to Eq. (51):

$$\mathbf{E}_\omega = \frac{1}{2\pi} \int_{-\infty}^{+\infty} \mathbf{E}(t) e^{i\omega t} dt. \quad (10.55)$$

In the particular case of radiation by a single point charge, we may use here the second (radiative) term of Eq. (19):

$$\mathbf{E}_\omega = \frac{1}{2\pi} \frac{q}{4\pi\epsilon_0} \frac{1}{cR} \int_{-\infty}^{+\infty} \left[\frac{\mathbf{n} \times \{(\mathbf{n} - \boldsymbol{\beta}) \times \dot{\boldsymbol{\beta}}\}}{(1 - \boldsymbol{\beta} \cdot \mathbf{n})^3} \right]_{\text{ret}} e^{i\omega t} dt. \quad (10.56)$$

Since the vectors \mathbf{n} and $\boldsymbol{\beta}$ are more natural functions of the radiation's emission (retarded) time t_{ret} , let us use Eqs. (5) and (16) to exclude the observation time t from this integral:

$$\mathbf{E}_\omega = \frac{q}{4\pi\epsilon_0} \frac{1}{2\pi} \frac{1}{cR} \int_{-\infty}^{+\infty} \left[\frac{\mathbf{n} \times \{(\mathbf{n} - \boldsymbol{\beta}) \times \dot{\boldsymbol{\beta}}\}}{(1 - \boldsymbol{\beta} \cdot \mathbf{n})^2} \right]_{\text{ret}} \exp\left\{i\omega\left(t_{\text{ret}} + \frac{R_{\text{ret}}}{c}\right)\right\} dt_{\text{ret}}. \quad (10.57)$$

Assuming that the observer is sufficiently far from the particle,¹⁸ we may treat the unit vector \mathbf{n} as a constant and also use the approximation (8.19) to reduce Eq. (57) to

¹⁵ Note that the expression under this integral differs from $d\mathcal{P}/d\Omega$ defined by Eq. (29) by the absence of the term $(1 - \boldsymbol{\beta} \cdot \mathbf{n}) = \partial t_{\text{ret}}/\partial t$ – see Eq. (16). This is natural because now we are calculating the wave energy arriving at the observation point \mathbf{r} during the time interval dt rather than dt_{ret} .

¹⁶ See, e.g. MA Eq. (14.4).

¹⁷ The notion of spectral density may be readily generalized to random processes – see, e.g., SM Sec. 5.4.

¹⁸ According to the estimate (49), for a synchrotron radiation pulse, this restriction requires the observer to be much farther than $\Delta r' \sim c\Delta t \sim R/\gamma^3$ from the particle. With the values $R \sim 10^4$ m and $\gamma \sim 10^5$ mentioned above, $\Delta r' \sim 10^{-11}$ m, so this requirement is satisfied for any realistic radiation detector.

$$\mathbf{E}_\omega = \frac{q}{4\pi\epsilon_0} \frac{1}{2\pi} \frac{1}{cR} \exp\left\{\frac{i\omega r}{c}\right\} \int_{-\infty}^{+\infty} \left[\frac{\mathbf{n} \times \{(\mathbf{n} - \boldsymbol{\beta}) \times \dot{\boldsymbol{\beta}}\}}{(1 - \boldsymbol{\beta} \cdot \mathbf{n})^2} \exp\left\{i\omega\left(t - \frac{\mathbf{n} \cdot \mathbf{r}'}{c}\right)\right\} \right]_{\text{ret}} dt_{\text{ret}}. \quad (10.58)$$

Plugging this expression into Eq. (54), and then using the definitions $c \equiv 1/(\epsilon_0\mu_0)^{1/2}$ and $Z_0 \equiv (\mu_0/\epsilon_0)^{1/2}$, we get¹⁹

$$I(\omega) = \frac{Z_0 q^2}{16\pi^3} \left| \int_{-\infty}^{+\infty} \left[\frac{\mathbf{n} \times \{(\mathbf{n} - \boldsymbol{\beta}) \times \dot{\boldsymbol{\beta}}\}}{(1 - \boldsymbol{\beta} \cdot \mathbf{n})^2} \exp\left\{i\omega\left(t - \frac{\mathbf{n} \cdot \mathbf{r}'}{c}\right)\right\} \right]_{\text{ret}} dt_{\text{ret}} \right|^2. \quad (10.59)$$

This result may be further simplified by noticing that the fraction before the exponent may be represented as a full derivative over t_{ret} ,

$$\left[\frac{\mathbf{n} \times \{(\mathbf{n} - \boldsymbol{\beta}) \times \dot{\boldsymbol{\beta}}\}}{(1 - \boldsymbol{\beta} \cdot \mathbf{n})^2} \right]_{\text{ret}} \equiv \left[\frac{\mathbf{n} \times \{(\mathbf{n} - \boldsymbol{\beta}) \times d\boldsymbol{\beta}/dt\}}{(1 - \boldsymbol{\beta} \cdot \mathbf{n})^2} \right]_{\text{ret}} \equiv \frac{d}{dt} \left[\frac{\mathbf{n} \times (\mathbf{n} \times \boldsymbol{\beta})}{1 - \boldsymbol{\beta} \cdot \mathbf{n}} \right]_{\text{ret}}, \quad (10.60)$$

and working out the resulting integral by parts. At this operation, the time differentiation of the parentheses in the exponent gives $d[t_{\text{ret}} - \mathbf{n} \cdot \mathbf{r}'(t_{\text{ret}})/c]/dt_{\text{ret}} = (1 - \mathbf{n} \cdot \mathbf{u}/c)_{\text{ret}} \equiv (1 - \boldsymbol{\beta} \cdot \mathbf{n})_{\text{ret}}$, leading to the cancellation of the remaining factor in the denominator and hence to a very simple general result:²⁰

$$I(\omega) = \frac{Z_0 q^2 \omega^2}{16\pi^3} \left| \int_{-\infty}^{+\infty} \left[\mathbf{n} \times (\mathbf{n} \times \boldsymbol{\beta}) \exp\left\{i\omega\left(t - \frac{\mathbf{n} \cdot \mathbf{r}'}{c}\right)\right\} \right]_{\text{ret}} dt_{\text{ret}} \right|^2. \quad (10.61)$$

Relativistic
radiation:
spectral
density

Now returning to the particular case of the synchrotron radiation, it is beneficial to choose the origin of time t_{ret} so that at $t_{\text{ret}} = 0$, the angle θ between the vectors \mathbf{n} and $\boldsymbol{\beta}$ takes its smallest value θ_0 , i.e., in terms of Fig. 5, the vector \mathbf{n} is within the $[y, z]$ -plane. Fixing this direction of the axes so that they do not move, we can redraw that figure as shown in Fig. 8.

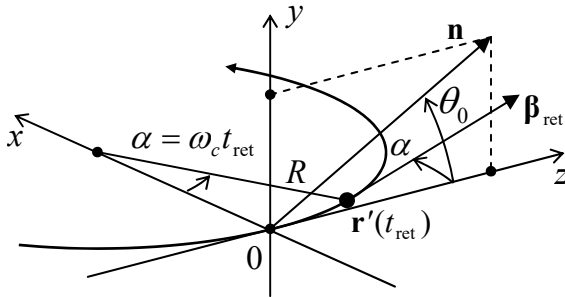


Fig. 10.8. Deriving the synchrotron radiation's spectral density. The vector \mathbf{n} is static within the $[y, z]$ -plane, while the vectors $\mathbf{r}'(t_{\text{ret}})$ and $\boldsymbol{\beta}_{\text{ret}}$ rotate, within the $[x, z]$ -plane, with the angular velocity ω_c of the particle.

In this “lab” reference frame, the vector \mathbf{n} does not depend on time, while the vectors $\mathbf{r}'(t_{\text{ret}})$ and $\boldsymbol{\beta}_{\text{ret}}$ do depend on it via the angle $\alpha \equiv \omega_c t_{\text{ret}}$:

¹⁹ Note that for our current purposes of calculation of the spectral density of radiation by a single particle, the factor $\exp\{i\omega r/c\}$ got canceled. However, as we have seen in Chapter 8, this factor plays a central role in the interference of radiation from several (many) sources. Such interference is important, in particular, in *undulators* and *free-electron lasers* – the devices to be (qualitatively) discussed below.

²⁰ Actually, this simplification is not occasional. According to Eq. (10b), the expression under the derivative in the last form of Eq. (60) is just the transverse component of the vector potential \mathbf{A} (give or take a constant factor), and from the discussion in Sec. 8.2 we know that this component determines the electric dipole radiation of a system, which dominates the radiation in our current case of a single particle with a non-zero electric charge.

$$\mathbf{n} = \{0, \sin \theta_0, \cos \theta_0\}, \quad \mathbf{r}'(t_{\text{ret}}) = \{R(1 - \cos \alpha), 0, R \sin \alpha\}, \quad \boldsymbol{\beta}_{\text{ret}} \equiv \{\beta \sin \alpha, 0, \beta \cos \alpha\}. \quad (10.62)$$

Now an easy multiplication yields

$$[\mathbf{n} \times (\mathbf{n} \times \boldsymbol{\beta})]_{\text{ret}} = \beta \{ \sin \alpha, \sin \theta_0 \cos \theta_0 \cos \alpha, -\sin^2 \theta_0 \sin \alpha \}, \quad (10.63)$$

$$\left[\exp \left\{ i\omega \left(t - \frac{\mathbf{n} \cdot \mathbf{r}'}{c} \right) \right\} \right]_{\text{ret}} = \exp \left\{ i\omega \left(t_{\text{ret}} - \frac{R}{c} \cos \theta_0 \sin \alpha \right) \right\}. \quad (10.64)$$

As we already know, in the (most interesting) ultra-relativistic limit $\gamma \gg 1$, most radiation is confined to short pulses, so only small angles $\alpha \sim \omega_c \Delta t_{\text{ret}} \sim \gamma^{-1}$ may contribute to the integral in Eq. (61). Moreover, since most radiation goes to small angles $\theta \sim \theta_0 \sim \gamma^{-1}$, it makes sense to consider only such small angles. Expanding both trigonometric functions of these small angles, participating in parentheses of Eq. (64), into the Taylor series, and keeping only the leading terms, we get

$$t_{\text{ret}} - \frac{R}{c} \cos \theta_0 \sin \alpha \approx t_{\text{ret}} - \frac{R}{c} \omega_c t_{\text{ret}} + \frac{R}{c} \frac{\theta_0^2}{2} \omega_c t_{\text{ret}} + \frac{R}{c} \frac{\omega_c^3}{6} t_{\text{ret}}^3. \quad (10.65)$$

Since $(R/c)\omega_c = u/c = \beta \approx 1$, in the two last terms, we may approximate this parameter by 1. However, it is crucial to distinguish the difference between the two first terms, proportional to $(1 - \beta)t_{\text{ret}}$, from zero; as we have done before, we may approximate it with $t_{\text{ret}}/2\gamma^2$. On the right-hand side of Eq. (63), which does not have such a critical difference, we may be bolder, taking²¹

$$\beta \{ \sin \alpha, \sin \theta_0 \cos \theta_0 \cos \alpha, -\sin^2 \theta_0 \sin \alpha \} \approx \{ \alpha, \theta_0, 0 \} \equiv \{ \omega_c t_{\text{ret}}, \theta_0, 0 \}. \quad (10.66)$$

As a result, Eq. (61) is reduced to

$$I(\omega) = \frac{Z_0 q^2}{16\pi^3} |a_x \mathbf{n}_x + a_y \mathbf{n}_y|^2 \equiv \frac{Z_0 q^2}{16\pi^3} (|a_x|^2 + |a_y|^2), \quad (10.67)$$

where a_x and a_y are the following dimensionless factors:

$$\begin{aligned} a_x &\equiv \omega \int_{-\infty}^{+\infty} \omega_c t_{\text{ret}} \exp \left\{ \frac{i\omega}{2} \left((\theta_0^2 + \gamma^{-2}) t_{\text{ret}} + \frac{\omega_c^2}{3} t_{\text{ret}}^3 \right) \right\} dt_{\text{ret}}, \\ a_y &\equiv \omega \int_{-\infty}^{+\infty} \theta_0 \exp \left\{ \frac{i\omega}{2} \left((\theta_0^2 + \gamma^{-2}) t_{\text{ret}} + \frac{\omega_c^2}{3} t_{\text{ret}}^3 \right) \right\} dt_{\text{ret}}, \end{aligned} \quad (10.68)$$

that describe the frequency spectra of two components of the synchrotron radiation, with mutually perpendicular polarization planes. Defining the following dimensionless parameter

$$\nu \equiv \frac{\omega}{3\omega_c} (\theta_0^2 + \gamma^{-2})^{3/2}, \quad (10.69)$$

²¹ This expression confirms that the in-plane (x) component of the electric field is an odd function of t_{ret} and hence of $t - t_0$ (see its sketch in Fig. 7b), while the normal (y) component is an even function of this difference. Also, note that for an observer exactly in the rotation plane ($\theta_0 = 0$) the latter component equals zero for all times – the fact which could be predicted from the very beginning because of the evident mirror symmetry of the problem with respect to the particle's rotation plane.

which is proportional to the observation frequency, and changing the integration variable to $\xi \equiv \omega_c t_{\text{ret}} / (\theta_0^2 + \gamma^{-2})^{1/2}$, the integrals (68) may be reduced to the modified Bessel functions of the second kind, but with fractional indices:

$$a_x = \frac{\omega}{\omega_c} (\theta_0^2 + \gamma^{-2}) \int_{-\infty}^{+\infty} \xi \exp\left\{\frac{3}{2} i \nu \left(\xi + \frac{\xi^3}{3}\right)\right\} d\xi = \frac{2\sqrt{3} i}{(\theta_0^2 + \gamma^{-2})^{1/2}} \nu K_{2/3}(\nu),$$

$$a_y = \frac{\omega}{\omega_c} \theta_0 (\theta_0^2 + \gamma^{-2})^{1/2} \int_{-\infty}^{+\infty} \exp\left\{\frac{3}{2} i \nu \left(\xi + \frac{\xi^3}{3}\right)\right\} d\xi = \frac{2\sqrt{3} \theta_0}{\theta_0^2 + \gamma^{-2}} \nu K_{1/3}(\nu)$$
(10.70)

Figure 9a shows the dependence of the Bessel factors defining the amplitudes a_x and a_y on the normalized observation frequency ν . It shows that the radiation intensity changes with frequency relatively slowly (note the log-log scale of the plot!) until the normalized frequency defined by Eq. (69) is increased beyond ~ 1 . For the most important observation angles $\theta_0 \sim \gamma$, this means that our estimate (50) is indeed correct, though formally the frequency spectrum extends to infinity.²²

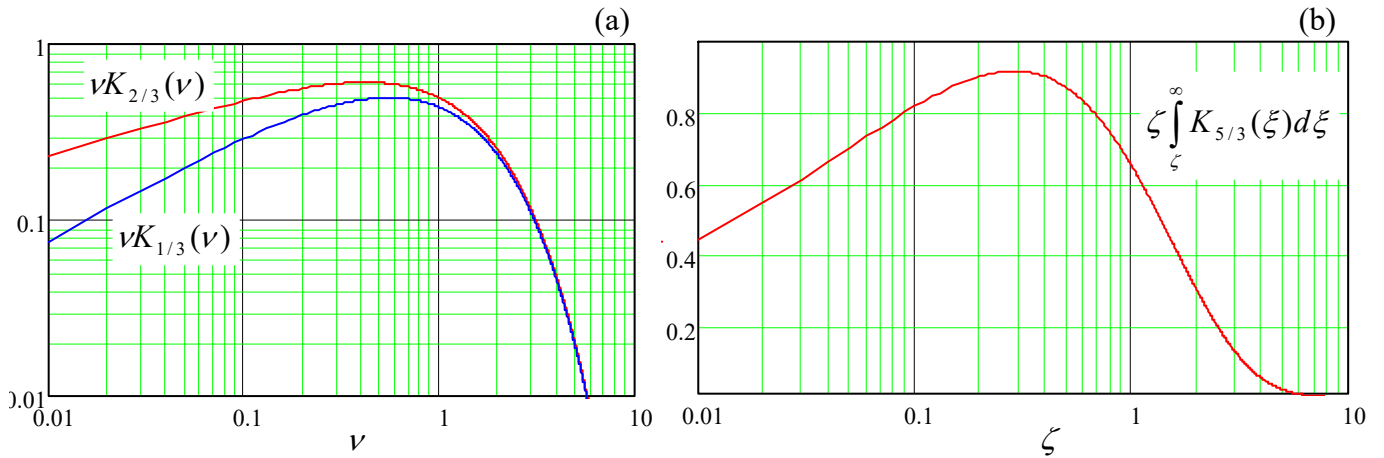


Fig. 10.9. The frequency spectra of: (a) two components of the synchrotron radiation, at a fixed angle θ_0 , and (b) its total (polarization- and angle-averaged) intensity.

Naturally, the spectral density integrated over the full solid angle exhibits a similar frequency behavior. Without performing the integration,²³ let me just give the result (also valid for $\gamma \gg 1$ only) for the reader's reference:

$$\oint_{4\pi} I(\omega) d\Omega = \frac{\sqrt{3}}{4\pi} q^2 \gamma^2 \int_{\zeta}^{\infty} K_{5/3}(\xi) d\xi, \quad \text{where } \zeta \equiv \frac{2}{3} \frac{\omega}{\omega_c \gamma^3}. \quad (10.71)$$

Figure 9b shows the dependence of this integral on the normalized frequency ζ . (This plot is sometimes called the “universal flux curve”.) In accordance with the estimate (50), it reaches the maximum at

²² The law of the spectral density decrease at large ν may be readily obtained from the second of Eqs. (2.158), which is valid even for any (even non-integer) Bessel function index n : $a_x \propto a_y \propto \nu^{1/2} \exp\{-\nu\}$. Here the exponential factor is certainly the most important one.

²³ For that, and many other details, the interested reader may be referred, for example, to the fundamental review collection by E. Koch *et al.* (eds.) *Handbook on Synchrotron Radiation* (in 5 vols.), North-Holland, 1983-1991, or to a more concise monograph by A. Hofmann, *The Physics of Synchrotron Radiation*, Cambridge U. Press, 2007.

$$\zeta_{\max} \approx 0.3, \quad \text{i.e. } \omega_{\max} \approx \frac{\omega_c}{2} \gamma^3. \quad (10.72)$$

For example, in the National Synchrotron Light Source (NSLS-II) in the Brookhaven National Laboratory near our SBU campus, with its ring's circumference of 792 m, the electron revolution period \mathcal{T} is 2.64 μs . With $\omega_c = 2\pi/\mathcal{T} \approx 2.4 \times 10^6 \text{ s}^{-1}$, for the achieved $\gamma \approx 6 \times 10^3$ ($\mathcal{E} \approx 3 \text{ GeV}$), we get $\omega_{\max} \sim 3 \times 10^{17} \text{ s}^{-1}$, i.e. the photon energy $\hbar\omega_{\max} \sim 200 \text{ eV}$ corresponding to soft X-rays. In light of this estimate, the reader may be surprised by Fig. 10, which shows the calculated spectra of the radiation that this facility was designed to produce, with the intensity maxima at photon energies up to a few keV.

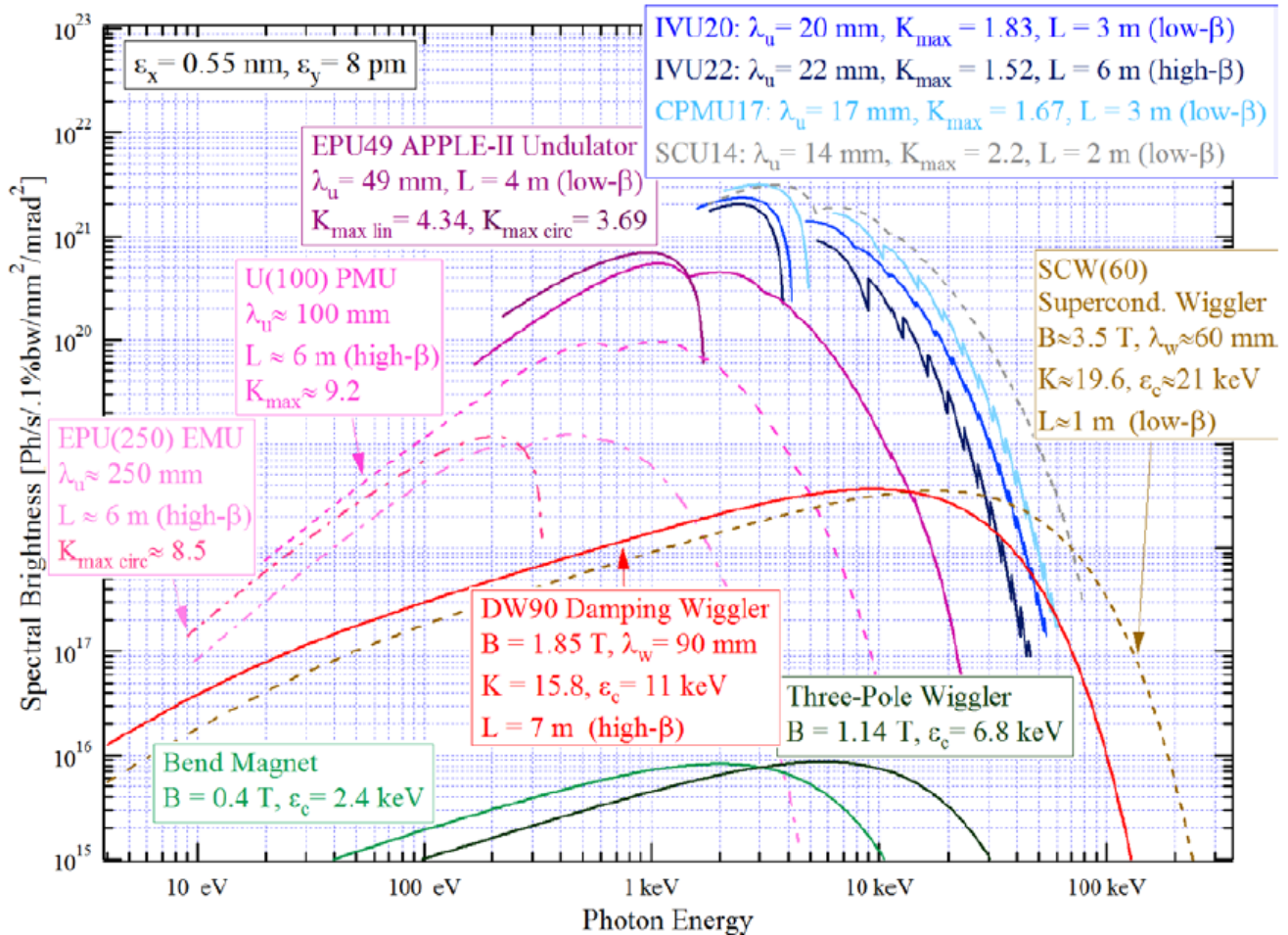


Fig. 10.10. Design brightness of various synchrotron radiation sources of the NSLS-II facility. For the bend magnets and wigglers, the “brightness” may be obtained by multiplication of the one-pulse spectral density $I(\omega)$ calculated above, by the number of electrons passing the source per second. (Note the non-SI units used by the synchrotron radiation community.) However, for undulators, there is an additional factor due to the partial coherence of radiation – see below. (Adapted from the document *NSLS-II Source Properties and Floor Layout* that was available online at <https://www.bnl.gov/ps/docs/pdf/SourceProperties.pdf> in 2011-2020.)

The reason for this discrepancy is that in the NSLS-II, and in all modern synchrotron light sources, most radiation is produced not by the circular orbit itself (which is, by the way, not exactly

circular, but consists of a series of straight and bend-magnet sections), but by such bend sections, and the devices called *wigglers* and *undulators*: strings of several strong magnets with alternating field direction (Fig. 11), that induce periodic bending (wiggling”) of the electron’s trajectory, with the synchrotron radiation emitted at each bend.

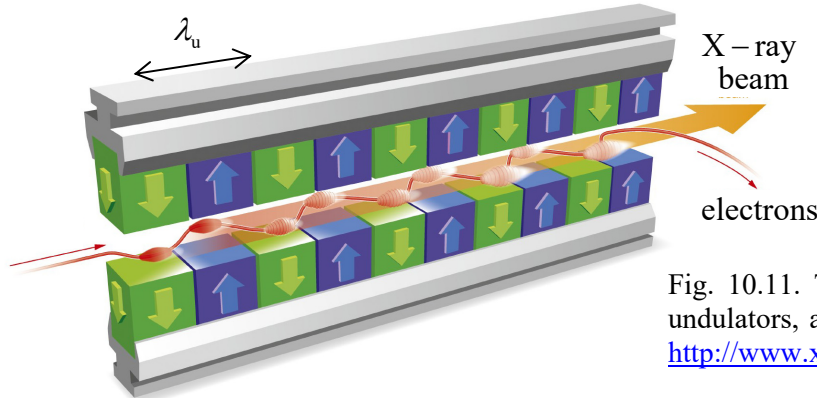


Fig. 10.11. The generic structure of the wigglers, undulators, and free-electron lasers. (Adapted from http://www.xfel.eu/overview/how_does_it_work/.)

The difference between the wigglers and the undulators is more quantitative than qualitative: the former devices have a larger spatial period λ_u (the distance between the adjacent magnets of the same polarity, see Fig. 11), giving enough space for the electron beam to bend by an angle larger than γ^{-1} , i.e. larger than the radiation cone’s width. As a result, the radiation reaches an in-plane observer as a periodic sequence of individual pulses – see Fig. 12a.

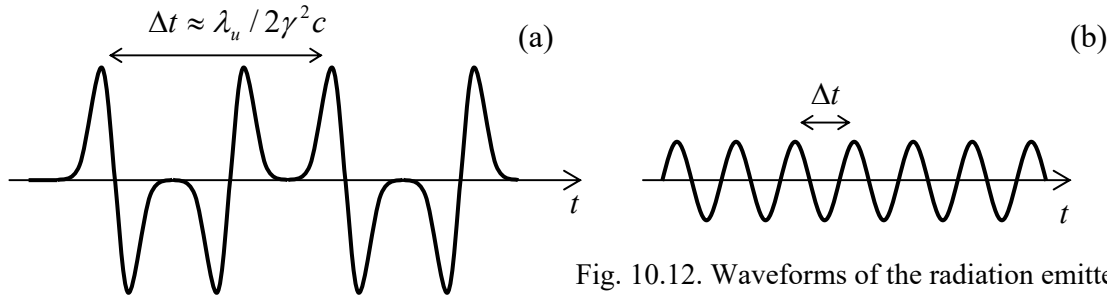


Fig. 10.12. Waveforms of the radiation emitted by (a) a wiggler and (b) an undulator – schematically.

The shape of each pulse, and hence its frequency spectrum, are essentially similar to those discussed above,²⁴ but with much higher local values of ω_c and hence ω_{\max} – see Fig. 10. Another difference is a much higher frequency of the pulses. Indeed, the fundamental Eq. (16) allows us to calculate the time distance between them, for the observer, as

$$\Delta t \approx \frac{\partial t}{\partial t_{\text{ret}}} \Delta t_{\text{ret}} \approx (1 - \beta) \frac{\lambda_u}{u} \approx \frac{1}{2\gamma^2} \frac{\lambda_u}{c} \ll \frac{\lambda_u}{c}, \quad (10.73)$$

²⁴ Indeed, the period λ_u is typically a few centimeters (see the numbers in Fig. 10), i.e. is much larger than the interval $\Delta r' \sim R/\gamma^3$ estimated above. Hence the synchrotron radiation results may be applied locally, to each electron beam’s bend. (In this context, a simple problem for the reader: use Eqs. (19) and (63) to explain the difference between shapes of the in-plane electric field pulses emitted at opposite magnetic poles of the wiggler, which is schematically shown in Fig. 12a.)

where the first two relations are valid at $\lambda_u \ll R$ (the relation typically satisfied very well, see the numbers in Fig. 10), and the last two relations assume the ultra-relativistic limit. As a result, the radiation intensity, which is proportional to the number of poles, is much higher than that from the bend magnets – see Fig. 10 again.

The situation is different in undulators – similar structures with a smaller spatial period λ_u , in which the electron’s velocity vector oscillates with an angular amplitude smaller than γ^{-1} . As a result, the radiation pulses overlap (Fig. 12b), and the radiation waveform is closer to the sinusoidal one. As a result, the radiation spectrum narrows to the central frequency²⁵

$$\omega_0 = \frac{2\pi}{\Delta t} \approx 2\gamma^2 \frac{2\pi c}{\lambda_u}. \quad (10.74)$$

For example, for the LSNL-II undulators with $\lambda_u = 2$ cm, this formula predicts a radiation peak at photon energy $\hbar\omega_0 \approx 4$ keV, in reasonable agreement with the quantitative calculation results shown in Fig. 10.²⁶ Due to the spectrum narrowing, the undulator’s radiation intensity is higher than that of wigglers using the same electron beam.

This spectrum-narrowing trend is brought to its logical conclusion in the so-called *free-electron lasers*²⁷ whose basic structure is the same as that of wigglers and undulators (Fig. 11), but the radiation at each beam bend is so intense and narrow-focused that it affects the electron motion downstream of the radiation cone. As a result, the radiation spectrum narrows around the central frequency (74), and its power grows as a square of the number N of electrons in the structure (rather than proportionately to N in wigglers and undulators).

Finally, note that wigglers, undulators, and free-electron lasers may be also used at the end of a linear electron accelerator (such as SLAC) which, as was noted above, may provide extremely high values of γ , and hence radiation frequencies, due to the smallness of radiation energy losses at the electron acceleration stage. Very unfortunately, I do not have time/space to discuss the (very interesting) physics of these devices in more detail.²⁸

10.4. Bremsstrahlung and Coulomb losses

Surprisingly, a very similar mechanism of radiation by charged particles works on a much smaller spatial scale, namely at their scattering by charged particles of the propagation medium. This

²⁵ This important formula may be also derived in the following way. Due to the relativistic length contraction (9.20), the undulator structure period as perceived by beam electrons is $\lambda' = \lambda_u/\gamma$, so the central frequency of the radiation in the reference frame moving with the electrons is $\omega_0' = 2\pi c/\lambda' = 2\pi c\gamma/\lambda_u$. For the lab-frame observer, this frequency is Doppler-upshifted in accordance with Eq. (9.44): $\omega_0 = \omega_0' [(1 + \beta)/(1 - \beta)]^{1/2} \approx 2\gamma\omega_0'$, giving the same result as Eq. (74).

²⁶ Some of the difference is due to the fact that those plots show the spectral density of the number of *photons* $n = \mathcal{E}/\hbar\omega$ per second, which peaks at a frequency below that of the density of power, i.e. of the *energy* \mathcal{E} per second.

²⁷ This name is somewhat misleading, because in contrast to the usual (“quantum”) lasers, a free-electron laser is essentially a classical device, and the dynamics of electrons in it is very similar to that in vacuum-tube microwave generators, such as the magnetrons briefly discussed in Sec. 9.6.

²⁸ The interested reader may be referred, for example, to either P. Luchini and H. Motz, *Undulators and Free-electron Lasers*, Oxford U. Press, 1990; or E. Salin *et al.*, *The Physics of Free Electron Lasers*, Springer, 2000.

effect, traditionally called by its German name *bremsstrahlung* (“brake radiation”), is responsible, in particular, for the continuous part of the frequency spectrum of the radiation produced in standard vacuum X-ray tubes, at the electron collisions with a metallic “anticathode”.²⁹

The bremsstrahlung in condensed matter is generally a rather complicated phenomenon because of the simultaneous involvement of many particles, and (frequently) some quantum electrodynamic effects. This is why I will give only a very brief glimpse at the theoretical description of this effect, for the simplest case when the scattering of incoming, relatively light charges (such as electrons, protons, α -particles, etc.) is produced by atomic nuclei, which remain virtually immobile during the scattering event (Fig. 13a). This is a reasonable approximation if the energy of incoming particles is not too low; otherwise, most scattering is produced by atomic electrons whose dynamics is substantially quantum – see below.

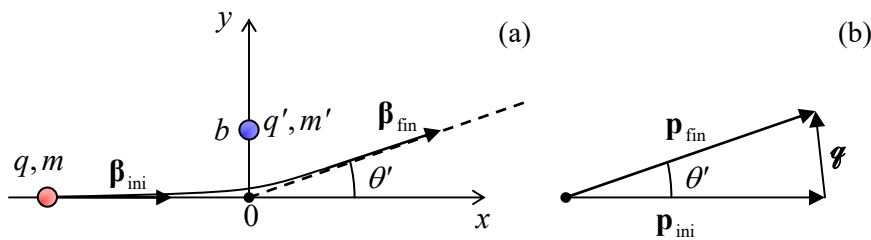


Fig. 10.13. The basic geometry of the bremsstrahlung and the Coulomb loss problems in the (a) direct and (b) reciprocal spaces.

To calculate the frequency spectrum of the radiation emitted during a single scattering event, it is convenient to use a byproduct of the last section’s analysis, namely Eq. (59) with the replacement (60):³⁰

$$I(\omega) = \frac{q^2}{4\pi\epsilon_0} \frac{1}{4\pi^2 c} \left| \int_{-\infty}^{+\infty} \left[\frac{d}{dt} \frac{\mathbf{n} \times (\mathbf{n} \times \boldsymbol{\beta})}{1 - \boldsymbol{\beta} \cdot \mathbf{n}} \exp\left\{i\omega\left(t - \frac{\mathbf{n} \cdot \mathbf{r}'}{c}\right)\right\} \right]_{\text{ret}} dt_{\text{ret}} \right|^2. \quad (10.75)$$

A typical duration τ of a single scattering event we are discussing is of the order of $\tau \equiv a_0/c \sim (10^{-10} \text{ m})/(3 \times 10^8 \text{ m/s}) \sim 10^{-18} \text{ s}$ in solids, and only an order of magnitude longer in gases at ambient conditions. This is why for most frequencies of interest, from zero all the way up to at least soft X-rays,³¹ we can use the so-called *low-frequency approximation*, taking the exponent in Eq. (75) for 1 through the whole collision event, i.e. the integration interval. This approximation immediately yields

$$I(\omega) = \frac{q^2}{4\pi\epsilon_0} \frac{1}{4\pi^2 c} \left| \frac{\mathbf{n} \times (\mathbf{n} \times \boldsymbol{\beta}_{\text{fin}})}{1 - \boldsymbol{\beta}_{\text{fin}} \cdot \mathbf{n}} - \frac{\mathbf{n} \times (\mathbf{n} \times \boldsymbol{\beta}_{\text{ini}})}{1 - \boldsymbol{\beta}_{\text{ini}} \cdot \mathbf{n}} \right|^2. \quad (10.76)$$

Bremsstrahlung:
single
collision

²⁹ Such X-ray radiation had been first observed experimentally (though not correctly interpreted) by N. Tesla in 1887, i.e. before it was rediscovered and studied in detail by W. Röntgen.

³⁰ In publications on this topic (whose development peak was in the 1920s-1930s), the Gaussian units are more common, and the uppercase letter Z is usually reserved for expressing charges as multiples of the fundamental charge e , rather than for the wave impedance. This is why, in order to avoid confusion and facilitate the comparison with other texts, in this section I (while still staying with the SI units used throughout my series) will use the fraction $1/\epsilon_0 c$, instead of its equivalent Z_0 , for the free-space wave impedance, and write the coefficients in a form that makes the transfer to the Gaussian units elementary: it is sufficient to replace all $(qq'/4\pi\epsilon_0)_{\text{SI}}$ with $(qq')_{\text{Gaussian}}$. In the (rare) cases when I spell out the charge values, I will use a different font: $q \equiv \mathfrak{F}e$, $q' \equiv \mathfrak{F}'e$.

³¹ A more careful analysis shows that this approximation is actually quite reasonable up to much higher frequencies, of the order of γ^2/τ .

In the non-relativistic limit ($\beta_{\text{ini}}, \beta_{\text{fin}} \ll 1$), this formula is reduced to the following result:

$$I(\omega) = \frac{q^2}{4\pi\epsilon_0} \frac{1}{4\pi^2 c} \frac{\mathcal{q}^2}{m^2 c^2} \sin^2 \theta \quad (10.77)$$

(which may be derived from Eq. (8.27) as well), where \mathcal{q} is the momentum transferred from the scattering center to the scattered charge (Fig. 13b):³²

$$\mathcal{q} \equiv \mathbf{p}_{\text{fin}} - \mathbf{p}_{\text{ini}} = m\Delta\mathbf{u} = mc\Delta\boldsymbol{\beta} = mc(\boldsymbol{\beta}_{\text{fin}} - \boldsymbol{\beta}_{\text{ini}}), \quad (10.78)$$

and θ (not to be confused with the particle scattering angle θ' shown in Fig. 13!) is the angle between the vector \mathcal{q} and the direction \mathbf{n} toward the observer – at the collision moment.

The most important feature of the result (77)-(78) is the frequency-independent (“white”) spectrum of the radiation, very typical for any rapid pulses that may be approximated as delta functions of time.³³ (Note, however, that Eq. (77) implies a fixed value of \mathcal{q} , so the statistics of this parameter, to be discussed in a minute, may “color” the radiation.)

Note also the “doughnut-shaped” angular distribution of the radiation, typical for non-relativistic systems, with the symmetry axis directed along the momentum transfer vector \mathcal{q} . In particular, this means that in typical cases when $|\theta'| \ll 1$, i.e. $\mathcal{q} \ll p$, when the vector \mathcal{q} is nearly normal to the vector \mathbf{p}_{ini} (see, e.g., the example shown in Fig. 13b), the bremsstrahlung produces a significant radiation flow in the direction back to the particle source – the fact significant for the operation of X-ray tubes.

Now integrating Eq. (77) over all wave propagation angles, just as we did for the instant radiation power in Sec. 8.2, we get the following spectral density of the particle energy loss,

$$-\frac{d\mathcal{E}}{d\omega} = \oint_{4\pi} I(\omega) d\Omega = \frac{2}{3\pi c} \frac{q^2}{4\pi^2 \epsilon_0} \frac{\mathcal{q}^2}{m^2 c^2}. \quad (10.79)$$

In most applications of the bremsstrahlung theory (as in most scattering problems³⁴), the impact parameter b (Fig. 13a), and hence the scattering angle θ' and the transferred momentum \mathcal{q} , have to be

³² Please note the font-marked difference between this variable (\mathcal{q}) and the particle’s electric charge (q).

³³ This is the basis, in particular, of the so-called *High-Harmonic Generation* (HHG) effect, discovered in 1977, which takes place at the irradiation of gases by intensive laser beams. The high electric field of the beam strips electrons from atoms, and accelerates them away from the remaining ions, just to slam them back into the same ions as the field’s polarity changes in time. The electrons change their momentum sharply during their recombination with the ions, resulting in bremsstrahlung-like emission of short radiation pulses. The spectrum of radiation from each such pulse obeys Eq. (77), but since the ionization/acceleration/recombination cycles repeat periodically with the frequency ω_0 of the laser field, the final spectrum consists of many equidistant lines, with frequencies $n\omega_0$. The classical theory of the bremsstrahlung does not give a cutoff $\omega_{\text{max}} = n_{\text{max}}\omega_0$ of the spectrum; such a limit is imposed by quantum mechanics: $\hbar\omega_{\text{max}} \approx \hbar\omega_{\text{max}} + 3\mathcal{E}_p$, where the so-called *ponderomotive energy* $\mathcal{E}_p = (eE_0/\omega_0)^2/4m_e$ is the average kinetic energy given to a free electron by the periodic electric field of the laser beam, with amplitude E_0 – see, for example, M. Lewenstein *et al.*, *Phys. Rev. A* **49**, 2117 (1994). In practice, the HHG pulses may be shorter than 10^{-15} s, and n_{max} as high as ~ 100 , enabling numerous applications of this effect.

³⁴ See, e.g., CM Sec. 3.5 and QM Sec. 3.3.

considered random. For elastic ($\beta_{\text{ini}} = \beta_{\text{fin}} \equiv \beta$) Coulomb collisions we can use the so-called *Rutherford formula* for the differential cross-section of scattering³⁵

$$\frac{d\sigma}{d\Omega'} = \left(\frac{qq'}{4\pi\epsilon_0} \right)^2 \left(\frac{1}{2pc\beta} \right)^2 \frac{1}{\sin^4(\theta'/2)}. \quad (10.80)$$

Here $d\sigma = 2\pi b db$ is the elementary area of the sample cross-section (as visible from the direction of the incident particles) corresponding to their scattering into an elementary body angle³⁶

$$d\Omega' = 2\pi \sin \theta' |d\theta'|. \quad (10.81)$$

Differentiating the geometric relation, which is evident from Fig. 13b,

$$q = 2p \sin \frac{\theta'}{2}, \quad (10.82)$$

we may represent Eq. (80) in a more convenient form

$$\frac{d\sigma}{dq} = 8\pi \left(\frac{qq'}{4\pi\epsilon_0} \right)^2 \frac{1}{u^2 q^3}. \quad (10.83)$$

Now combining Eqs. (79) and (83), we get

$$-\frac{d\mathcal{E}}{d\omega} \frac{d\sigma}{dq} = \frac{16}{3} \frac{q^2}{4\pi\epsilon_0} \left(\frac{qq'}{4\pi\epsilon_0 mc^2} \right)^2 \frac{1}{c\beta^2} \frac{1}{q}. \quad (10.84)$$

This product is called the *differential radiation cross-section*. When integrated over all values of q (which is equivalent to averaging over all values of the impact parameter), it gives a convenient measure of the radiation intensity. Indeed, after the multiplication by the volume density n of independent scattering centers, such integral yields the particle's energy loss per unit bandwidth of radiation per unit path length, $-d^2\mathcal{E}/d\omega dx$. A minor problem here is that the integral of $1/q$ formally diverges at both infinite and zero values of q . However, these divergences are very weak (logarithmic), and the integral converges due to virtually any reason unaccounted for in our simple analysis. The standard (though slightly approximate) way to account for these effects is to write

$$-\frac{d^2\mathcal{E}}{d\omega dx} \approx \frac{16}{3} n \frac{q^2}{4\pi\epsilon_0} \left(\frac{qq'}{4\pi\epsilon_0 mc^2} \right)^2 \frac{1}{c\beta^2} \ln \frac{q_{\text{max}}}{q_{\text{min}}}, \quad (10.85)$$

and then plug, instead of q_{max} and q_{min} , the scales of the most important effects limiting the range of the transferred momentum's magnitude. In the classical-mechanics analysis, according to Eq. (82), $q_{\text{max}} = 2p \equiv 2mu$. To estimate q_{min} , let us note that the very small momentum transfer takes place when the impact parameter b is very large, and hence the effective scattering time $\tau \sim b/v$ is very long. Recalling the condition of the low-frequency approximation, we may associate q_{min} with $\tau \sim 1/\omega$ and hence with $b \sim$

³⁵ See, e.g., CM Eq. (3.73) with $\alpha = qq'/4\pi\epsilon_0$. In the form used in Eq. (80), the Rutherford formula is also valid for the small-angle scattering of relativistic particles, the criterion being $|\Delta\beta| \ll 2/\gamma$.

³⁶ Again, the angle θ' and the differential $d\Omega'$, describing the scattered *particles* (see Fig. 13) should not be confused with the parameters θ and $d\Omega$ describing the *radiation* emitted at the scattering event.

$u\tau \sim v/\omega$. Since for the small scattering angles, q is close to the impulse $F\tau \sim (qq'/4\pi\epsilon_0 b^2)\tau$ of the Coulomb force, we get the estimate $q_{\min} \sim (qq'/4\pi\epsilon_0)\omega/u^2$, and Eq. (85) should be used with

$$\ln \frac{q_{\max}}{q_{\min}} = \ln \left(\frac{2mu^3}{\omega} \bigg/ \frac{qq'}{4\pi\epsilon_0} \right). \quad (10.86)$$

Classical
brems-
strahlung

This is *Bohr's formula* for what is called the *classical bremsstrahlung*. We see that the low momentum cutoff indeed makes the spectrum slightly colored, with more energy going to lower frequencies. There is even a formal divergence at $\omega \rightarrow 0$; however, this divergence is integrable, so it does not present a problem for finding the total energy radiative losses ($-d\mathcal{E}/dx$) as an integral of Eq. (86) over all radiated frequencies ω . A larger problem for this procedure is the upper integration limit, $\omega \rightarrow \infty$, at which the integral diverges. This means that our approximate description, which considers the collision as an elastic process, becomes invalid and needs to be amended by taking into account the difference between the initial and final kinetic energies of the particle due to radiation of the energy quantum $\hbar\omega$ of the emitted photon, so

$$\frac{p_{\text{ini}}^2}{2m} - \frac{p_{\text{fin}}^2}{2m} = \hbar\omega, \quad \text{i.e. } \frac{p_{\text{ini}}^2}{2m} = \mathcal{E}, \quad \frac{p_{\text{fin}}^2}{2m} = \mathcal{E} - \hbar\omega, \quad . \quad (10.87)$$

As a result, taking into account that the minimum and maximum values of q correspond to, respectively, the parallel and antiparallel alignments of the vectors \mathbf{p}_{ini} and \mathbf{p}_{fin} , we get

$$\ln \frac{q_{\max}}{q_{\min}} = \ln \frac{p_{\text{ini}} + p_{\text{fin}}}{p_{\text{ini}} - p_{\text{fin}}} \equiv \ln \frac{(p_{\text{ini}} + p_{\text{fin}})^2 / 2m}{(p_{\text{ini}}^2 - p_{\text{fin}}^2) / 2m} = \ln \frac{[\mathcal{E}^{1/2} + (\mathcal{E} - \hbar\omega)^{1/2}]^2}{\hbar\omega}, \quad (10.88)$$

Quantum
brems-
strahlung

Plugged into Eq. (85), this expression yields the so-called *Bethe-Heitler formula* for *quantum bremsstrahlung*.³⁷ Note that in this approach, q_{\max} is close to that of the classical approximation, but q_{\min} is of the order of $\hbar\omega/u$, so

$$\frac{q_{\min}|_{\text{classical}}}{q_{\min}|_{\text{quantum}}} \sim \frac{\alpha \mathcal{F} \mathcal{F}'}{\beta}, \quad (10.89)$$

where \mathcal{F} and \mathcal{F}' are the particles' charges in the units of e , and α is the dimensionless *fine structure* (“Sommerfeld”) *constant*,

$$\alpha \equiv \frac{e^2}{4\pi\epsilon_0 \hbar c} \Big|_{\text{SI}} = \frac{e^2}{\hbar c} \Big|_{\text{Gaussian}} \approx \frac{1}{137} \ll 1, \quad (10.90)$$

which is one of the basic notions of quantum mechanics.³⁸ Due to the smallness of the constant, the ratio (89) is below 1 for most cases of practical interest, and since the integral of (84) over q is limited by the largest of all possible cutoffs q_{\min} , it is the Bethe-Heitler formula that should be used.

³⁷ The modifications of this formula necessary for the relativistic description are surprisingly minor – see, e.g., Chapter 15 in J. Jackson, *Classical Electrodynamics*, 3rd ed., Wiley 1999. For even more detail, the standard reference monograph on bremsstrahlung is W. Heitler, *The Quantum Theory of Radiation*, 3rd ed., Oxford U. Press 1954 (reprinted in 1984 and 2010 by Dover).

³⁸ See, e.g., QM Secs. 4.4, 6.3, 6.4, 9.3, 9.5, and 9.7.

Now nothing prevents us from calculating the total radiative losses of energy per unit length:

$$-\frac{d\mathcal{E}}{dx} = \int_0^{\infty} \left(-\frac{d^2\mathcal{E}}{d\omega dz} \right) d\omega = \frac{16}{3} n \frac{q^2}{4\pi\epsilon_0 c} \left(\frac{qq'}{4\pi\epsilon_0 mc^2} \right)^2 \frac{1}{\beta^2} 2 \int_0^{\omega_{\max}} \ln \frac{\mathcal{E}^{1/2} - (\mathcal{E} - \hbar\omega)^{1/2}}{(\hbar\omega)^{1/2}} d\omega, \quad (10.91)$$

where $\hbar\omega_{\max} = \mathcal{E}$ is the maximum energy of the radiation quantum. By introducing the dimensionless integration variable $\xi \equiv \hbar\omega/\mathcal{E} = 2\hbar\omega/(mu^2/2)$, this integral is reduced to a table one,³⁹ and we get

$$-\frac{d\mathcal{E}}{dx} = \frac{16}{3} n \frac{q^2}{4\pi\epsilon_0 c} \left(\frac{qq'}{4\pi\epsilon_0 mc^2} \right)^2 \frac{1}{\beta^2} \frac{u^2}{\hbar} \equiv \frac{16}{3} n \left(\frac{q'^2}{4\pi\epsilon_0 \hbar c} \right) \left(\frac{q^2}{4\pi\epsilon_0} \right)^2 \frac{1}{mc^2}. \quad (10.92)$$

Following my usual style, at this point I would give you an estimate of the losses for a typical case; however, let me first discuss a parallel particle energy loss mechanism, the so-called *Coulomb losses*, due to the transfer of mechanical impulse from the scattered particle to the scattering centers. (This energy eventually goes into an increase of the thermal energy of the scattering medium, rather than to the electromagnetic radiation.)

Using Eqs. (9.139) for the electric field of a linearly moving charge q , we can readily find the momentum it transfers to the counterpart charge q' :⁴⁰

$$\Delta p' = |(\Delta p')_y| = \left| \int_{-\infty}^{+\infty} (\dot{p}')_y dt \right| = \left| \int_{-\infty}^{+\infty} q'E_y dt \right| = \frac{qq'}{4\pi\epsilon_0} \int_{-\infty}^{+\infty} \frac{\gamma b}{(b^2 + \gamma^2 u^2 t^2)^{3/2}} dt = \frac{qq'}{4\pi\epsilon_0} \frac{2}{bu}. \quad (10.93)$$

Hence, the kinetic energy acquired by the scattering particle (and hence to the loss of the energy \mathcal{E} of the incident particle) is

$$-\Delta\mathcal{E} = \frac{(\Delta p')^2}{2m'} = \left(\frac{qq'}{4\pi\epsilon_0} \right)^2 \frac{2}{m'u^2 b^2}. \quad (10.94)$$

Such elementary energy losses have to be summed up over all collisions, with random values of the impact parameter b . At the scattering center density n , the number of collisions per small path length dx per small range db is $dN = n 2\pi b db dx$, so

Coulomb
losses

$$-\frac{d\mathcal{E}}{dx} = -\int \Delta\mathcal{E} dN = n \left(\frac{qq'}{4\pi\epsilon_0} \right)^2 \frac{2}{m'u^2} 2\pi \int_{b_{\min}}^{b_{\max}} \frac{db}{b} = 4\pi n \left(\frac{qq'}{4\pi\epsilon_0} \right)^2 \frac{\ln B}{m'u^2}, \quad \text{where } B \equiv \frac{b_{\max}}{b_{\min}}. \quad (10.95)$$

Here, at the last step, the logarithmic integral over b was treated similarly to that over q in the bremsstrahlung theory. This approximation is adequate because the ratio b_{\max}/b_{\min} is much larger than 1. Indeed, b_{\min} may be estimated from $(\Delta p')_{\max} \sim p = \gamma mu$. For this value, Eq. (93) with $q' \sim q$ gives $b_{\min} \sim r_c$ (see Eq. (8.41) and its discussion), which, for elementary particles, is of the order of 10^{-15} m. On the other hand, for the most important case when the Coulomb energy absorbers are electrons (which, according to Eq. (94), are the most efficient ones, due to their very low mass m'), b_{\max} may be estimated from the condition $\tau = b/\gamma u \sim 1/\omega_{\min}$, where $\omega_{\min} \sim 10^{16}$ s⁻¹ is the characteristic frequency of electron

³⁹ See, e.g., MA Eq. (6.14).

⁴⁰ According to Eq. (9.139), $E_z = 0$, while the net impulse of the longitudinal force $q'E_x$ is zero, so Eq. (93) gives the full momentum transfer.

transitions in atoms. (Quantum mechanics forbids such energy transfer at lower frequencies.) From here, we have the estimate $b_{\max} \sim \gamma u / \omega_{\min}$, so

$$B \equiv \frac{b_{\max}}{b_{\min}} \sim \frac{\gamma u}{r_c \omega_{\min}}, \quad (10.96)$$

for $\gamma \sim 1$ and $u \sim c \approx 3 \times 10^8$ m/s giving $b_{\max} \sim 3 \times 10^{-8}$ m, so $B \sim 10^9$ (give or take a couple of orders of magnitude – this does not change the estimate $\ln B \approx 20$ too much).⁴¹

Now we can compare the non-radiative Coulomb losses (95) with the radiative losses due to the bremsstrahlung, given by Eq. (92):

$$\frac{-d\mathcal{E}|_{\text{radiation}}}{-d\mathcal{E}|_{\text{Coulomb}}} \sim \alpha \mathcal{F} \mathcal{F}' \frac{m'}{m} \beta^2 \frac{1}{\ln B}, \quad (10.97)$$

Since $\alpha \sim 10^{-2} \ll 1$, for non-relativistic particles ($\beta \ll 1$) the bremsstrahlung losses of energy are much lower (that is why I did not want to rush with their estimates), and only for ultra-relativistic particles, the relation may be opposite.

According to Eqs. (95)-(96), for electron-electron scattering ($q = q' = -e$, $m = m' = m_e$),⁴² at the value $n = 6 \times 10^{26} \text{ m}^{-3}$ typical for air at ambient conditions, the characteristic length of energy loss,

$$l_c \equiv \frac{\mathcal{E}}{(-d\mathcal{E}/dx)}, \quad (10.98)$$

for electrons with kinetic energy $\mathcal{E} = 6$ keV is close to $2 \times 10^{-4} \text{ m} \equiv 0.2$ mm. (This is why we need high vacuum in electron microscope columns and other vacuum electron devices.) Since $l_c \propto \mathcal{E}^2$, more energetic particles penetrate to matter deeper, until the bremsstrahlung steps in, and limits this trend at very high energies.

10.5. Density effects and the Cherenkov radiation

For condensed matter, the Coulomb loss estimate made in the last section is not quite suitable, because it is based on the upper cutoff $b_{\max} \sim \gamma u / \omega_{\min}$. For the example given above, the incoming electron velocity u is close to 5×10^7 m/s, and for the typical value $\omega_{\min} \sim 10^{16} \text{ s}^{-1}$ ($\hbar \omega_{\min} \sim 10$ eV), this cutoff b_{\max} is of the order of $\sim 5 \times 10^{-9} \text{ m} = 5$ nm. Even for air at ambient conditions, this is somewhat larger than the average distance (~ 2 nm) between the molecules, so at the high end of the impact parameter range, at $b \sim b_{\max}$, the Coulomb loss events in adjacent molecules are not quite independent, and the theory needs some corrections. For condensed matter, with much higher particle density n , most collisions satisfy the following condition:

⁴¹ A quantum analysis (carried out by Hans Bethe in 1940) replaces, in Eq. (95), $\ln B$ with $\ln(2\gamma^2 m u^2 / \hbar \langle \omega \rangle) - \beta^2$, where $\langle \omega \rangle$ is the average frequency of the atomic quantum transitions weight by their oscillator strength. This refinement does not change the estimate given below. Note that both the classical and quantum formulas describe a fast increase (as $1/\beta$) of the energy loss rate ($-d\mathcal{E}/dx$) at $\gamma \rightarrow 1$, and its slow increase (as $\ln \gamma$) at $\gamma \rightarrow \infty$, so the losses have a minimum at $(\gamma - 1) \sim 1$.

⁴² Actually, the above analysis has neglected the change of momentum of the incident particle. This is legitimate at $m' \ll m$, but for $m = m'$ the change approximately doubles the energy losses. Still, this does not change the order of magnitude of the estimate.

$$nb^3 \gg 1, \quad (10.99)$$

and the treatment of Coulomb collisions as a set of independent events is inadequate. However, this condition enables the opposite approach: treating the medium as a continuum. In the time-domain formulation used in the previous sections of this chapter, this would be a very complex problem, because it would require an explicit description of the medium dynamics. Here the frequency-domain approach, based on the Fourier transform in both time and space, helps a lot, provided that the functions $\varepsilon(\omega)$ and $\mu(\omega)$ are considered known – either calculated or taken from experiment. Let us have a good look at this approach because it gives some interesting (and practically important) results.

In Chapter 6, we have used the macroscopic Maxwell equations to derive Eqs. (6.118), which describe the time evolution of electrodynamic potentials in a linear medium with frequency-independent ε and μ . Looking for all functions participating in Eqs. (6.118) in the plane-wave expansion form⁴³

$$f(\mathbf{r}, t) = \int d^3k \int d\omega f_{\mathbf{k}, \omega} e^{i(\mathbf{k} \cdot \mathbf{r} - \omega t)}, \quad (10.100)$$

and requiring all coefficients at similar exponents to be balanced, we get their Fourier images:⁴⁴

$$(k^2 - \omega^2 \varepsilon \mu) \phi_{\mathbf{k}, \omega} = \frac{\rho_{\mathbf{k}, \omega}}{\varepsilon}, \quad (k^2 - \omega^2 \varepsilon \mu) \mathbf{A}_{\mathbf{k}, \omega} = \mu \mathbf{j}_{\mathbf{k}, \omega}. \quad (10.101)$$

As was discussed in Chapter 7, in such a Fourier form, the macroscopic Maxwell theory remains valid even for dispersive (but isotropic and linear!) media, so Eqs. (101) may be generalized as

$$[k^2 - \omega^2 \varepsilon(\omega) \mu(\omega)] \phi_{\mathbf{k}, \omega} = \frac{\rho_{\mathbf{k}, \omega}}{\varepsilon(\omega)}, \quad [k^2 - \omega^2 \varepsilon(\omega) \mu(\omega)] \mathbf{A}_{\mathbf{k}, \omega} = \mu(\omega) \mathbf{j}_{\mathbf{k}, \omega}, \quad (10.102)$$

An evident advantage of these equations is that their formal solution is elementary:

$$\phi_{\mathbf{k}, \omega} = \frac{\rho_{\mathbf{k}, \omega}}{\varepsilon(\omega) [k^2 - \omega^2 \varepsilon(\omega) \mu(\omega)]}, \quad \mathbf{A}_{\mathbf{k}, \omega} = \frac{\mu(\omega) \mathbf{j}_{\mathbf{k}, \omega}}{[k^2 - \omega^2 \varepsilon(\omega) \mu(\omega)]}, \quad (10.103)$$

Field potentials in a linear medium

so the “only” remaining things to do is, first, to calculate the Fourier transforms of the functions $\rho(\mathbf{r}, t)$ and $\mathbf{j}(\mathbf{r}, t)$, describing stand-alone charges and currents, using the transform reciprocal to Eq. (100), with one factor $1/2\pi$ per each scalar dimension,

$$f_{\mathbf{k}, \omega} = \frac{1}{(2\pi)^4} \int d^3r \int dt f(\mathbf{r}, t) e^{-i(\mathbf{k} \cdot \mathbf{r} - \omega t)}, \quad (10.104)$$

and then to carry out the integration (100) of Eqs. (103).

For our problem of a single charge q uniformly moving through a medium with velocity \mathbf{u} ,

$$\rho(\mathbf{r}, t) = q \delta(\mathbf{r} - \mathbf{u}t), \quad \mathbf{j}(\mathbf{r}, t) = q \mathbf{u} \delta(\mathbf{r} - \mathbf{u}t), \quad (10.105)$$

⁴³ All integrals here and below are in infinite limits unless specified otherwise.

⁴⁴ As was discussed in Sec. 7.2, the Ohmic conductivity of the medium (generally, also a function of frequency) may be readily incorporated into the dielectric permittivity: $\varepsilon(\omega) \rightarrow \varepsilon_{\text{ef}}(\omega) + i\sigma(\omega)/\omega$. In this section, I will assume that such incorporation, which is especially natural for high frequencies, has been performed, so the current density $\mathbf{j}(\mathbf{r}, t)$ describes only stand-alone currents – for example, the current (105) of the incident particle.

the first task is easy:

$$\rho_{\mathbf{k},\omega} = \frac{q}{(2\pi)^4} \int d^3r \int dt q \delta(\mathbf{r} - \mathbf{u}t) e^{-i(\mathbf{k}\cdot\mathbf{r} - \omega t)} = \frac{q}{(2\pi)^4} \int e^{i(\omega t - \mathbf{k}\cdot\mathbf{u}t)} dt = \frac{q}{(2\pi)^3} \delta(\omega - \mathbf{k}\cdot\mathbf{u}). \quad (10.106)$$

Since the expressions (105) for $\rho(\mathbf{r}, t)$ and $\mathbf{j}(\mathbf{r}, t)$ differ only by a constant factor \mathbf{u} , it is clear that the absolutely similar calculation for the current gives

$$\mathbf{j}_{\mathbf{k},\omega} = \frac{q\mathbf{u}}{(2\pi)^3} \delta(\omega - \mathbf{k}\cdot\mathbf{u}). \quad (10.107)$$

Let us summarize what we have got by now, by plugging Eqs. (106)-(107) into Eqs. (103):

$$\phi_{\mathbf{k},\omega} = \frac{1}{(2\pi)^3} \frac{q\delta(\omega - \mathbf{k}\cdot\mathbf{u})}{\varepsilon(\omega)[k^2 - \omega^2\varepsilon(\omega)\mu(\omega)]}, \quad \mathbf{A}_{\mathbf{k},\omega} = \frac{1}{(2\pi)^3} \frac{\mu(\omega)q\mathbf{u}\delta(\omega - \mathbf{k}\cdot\mathbf{u})}{[k^2 - \omega^2\varepsilon(\omega)\mu(\omega)]} \equiv \varepsilon(\omega)\mu(\omega)\mathbf{u}\phi_{\mathbf{k},\omega}. \quad (10.108)$$

Now, at the last calculation step, namely the integration (100), we are starting to pay a heavy price for the easiness of the first steps. This is why let us think well about what exactly we need from it. First of all, for the calculation of power losses, the electric field is more convenient to use than the potentials, so let us calculate the Fourier images of \mathbf{E} and \mathbf{B} . Plugging the expansion (100) into the basic relations (6.7), and again requiring the balance of exponent's coefficients, we get

$$\mathbf{E}_{\mathbf{k},\omega} = -i\mathbf{k}\phi_{\mathbf{k},\omega} + i\omega\mathbf{A}_{\mathbf{k},\omega} = i[\omega\varepsilon(\omega)\mu(\omega)\mathbf{u} - \mathbf{k}]\phi_{\mathbf{k},\omega}, \quad \mathbf{B}_{\mathbf{k},\omega} = i\mathbf{k} \times \mathbf{A}_{\mathbf{k},\omega} = i\varepsilon(\omega)\mu(\omega)\mathbf{k} \times \mathbf{u}\phi_{\mathbf{k},\omega}, \quad (10.109)$$

so Eqs. (100) and (108) yield

$$\mathbf{E}(\mathbf{r}, t) = \int d^3k \int d\omega \mathbf{E}_{\mathbf{k},\omega} e^{i(\mathbf{k}\cdot\mathbf{r} - \omega t)} = \frac{iq}{(2\pi)^3} \int d^3k \int d\omega \frac{[\omega\varepsilon(\omega)\mu(\omega)\mathbf{u} - \mathbf{k}]\delta(\omega - \mathbf{k}\cdot\mathbf{u})}{\varepsilon(\omega)[k^2 - \omega^2\varepsilon(\omega)\mu(\omega)]} e^{i(\mathbf{k}\cdot\mathbf{r} - \omega t)}. \quad (10.110)$$

This formula may be rewritten as the temporal Fourier integral (51), with the following \mathbf{r} -dependent complex amplitude:

$$\mathbf{E}_\omega(\mathbf{r}) = \int \mathbf{E}_{\mathbf{k},\omega} e^{i\mathbf{k}\cdot\mathbf{r}} d^3k = \frac{iq}{(2\pi)^3} \int \frac{[\omega\varepsilon(\omega)\mu(\omega)\mathbf{u} - \mathbf{k}]\delta(\omega - \mathbf{k}\cdot\mathbf{u})}{\varepsilon(\omega)[k^2 - \omega^2\varepsilon(\omega)\mu(\omega)]} e^{i\mathbf{k}\cdot\mathbf{r}} d^3k. \quad (10.111)$$

Let us calculate the Cartesian components of this partial Fourier image \mathbf{E}_ω , at a point separated by distance b from the particle's trajectory. Selecting the coordinates and time origin as shown in Fig. 3, we have $\mathbf{r} = \{0, b, 0\}$ and $\mathbf{u} = \{u, 0, 0\}$, so only E_x and E_y are different from zero. In particular, according to Eq. (111),

$$(E_x)_\omega = \frac{iq}{(2\pi)^3 \varepsilon(\omega)} \int dk_x \int dk_y \int dk_z \frac{\omega\varepsilon(\omega)\mu(\omega)u - k_x}{k^2 - \omega^2\varepsilon(\omega)\mu(\omega)} \delta(\omega - k_x u) \exp\{ik_y b\}. \quad (10.112)$$

The delta function kills one integral (over k_x) of the three, and we get

$$(E_x)_\omega = \frac{iq}{(2\pi)^3 \varepsilon(\omega)u} \left[\omega\varepsilon(\omega)\mu(\omega)u - \frac{\omega}{u} \right] \int \exp\{ik_y b\} dk_y \int \frac{dk_z}{\omega^2/u^2 + k_y^2 + k_z^2 - \omega^2\varepsilon(\omega)\mu(\omega)}. \quad (10.113)$$

The internal integral (over k_z) may be readily reduced to the table integral $\int d\xi/(1 + \xi^2)$ in infinite limits, equal to π ,⁴⁵ and the result represented as

$$(E_x)_\omega = -\frac{i\pi q\kappa^2}{(2\pi)^3 \omega \varepsilon(\omega)} \int \frac{\exp\{ik_y b\}}{(k_y^2 + \kappa^2)^{1/2}} dk_y, \quad (10.114)$$

where the parameter κ (generally, a complex function of frequency) is defined as⁴⁶

Function $\kappa(\omega)$

$$\kappa^2(\omega) \equiv \omega^2 \left[\frac{1}{u^2} - \varepsilon(\omega)\mu(\omega) \right]. \quad (10.115)$$

The last integral may be expressed via the modified Bessel function of the second kind:⁴⁷

$$(E_x)_\omega = -\frac{iqu\kappa^2}{(2\pi)^2 \omega \varepsilon(\omega)} K_0(\kappa b). \quad (10.116)$$

A very similar calculation yields

$$(E_y)_\omega = \frac{q\kappa}{(2\pi)^2 \varepsilon(\omega)} K_1(\kappa b). \quad (10.117)$$

Now, instead of rushing to make the final integration (51) over ω to calculate $\mathbf{E}(t)$, let us realize that what we need most is the total energy loss through the whole time of the particle's passage over an elementary distance dx . According to Eq. (4.38), the energy loss per unit volume is

$$-\frac{d\mathcal{E}}{dV} = \int \mathbf{j} \cdot \mathbf{E} dt, \quad (10.118)$$

where \mathbf{j} is the current of the bound charges in the medium, and should not be confused with the stand-alone incident-particle current (105). This integral may be readily expressed via the partial Fourier image \mathbf{E}_ω and the similarly defined image \mathbf{j}_ω , just as it was done at the derivation of Eq. (54):

$$-\frac{d\mathcal{E}}{dV} = \int dt \int d\omega e^{-i\omega t} \int d\omega' e^{-i\omega' t} \mathbf{j}_\omega \cdot \mathbf{E}_{\omega'} = 2\pi \int d\omega \int d\omega' \mathbf{j}_\omega \cdot \mathbf{E}_{\omega'} \delta(\omega + \omega') = 2\pi \int \mathbf{j}_\omega \cdot \mathbf{E}_{-\omega} d\omega. \quad (10.119)$$

Let us incorporate the effective Ohmic conductivity $\sigma_{\text{ef}}(\omega)$ into the complex permittivity $\varepsilon(\omega)$ just as this was discussed in Sec. 7.2, using Eq. (7.46) to write

$$\mathbf{j}_\omega = \sigma_{\text{ef}}(\omega) \mathbf{E}_\omega = -i\omega \varepsilon(\omega) \mathbf{E}_\omega. \quad (10.120)$$

As a result, Eq. (119) yields

$$-\frac{d\mathcal{E}}{dV} = -2\pi i \int \varepsilon(\omega) \mathbf{E}_\omega \cdot \mathbf{E}_{-\omega} \omega d\omega = 4\pi \text{Im} \int_0^\infty \varepsilon(\omega) |E_\omega|^2 \omega d\omega. \quad (10.121)$$

(The last step was possible due to the property $\varepsilon(-\omega) = \varepsilon^*(\omega)$, which was discussed in Sec. 7.2.)

⁴⁵ See, e.g., MA Eq. (6.5a).

⁴⁶ The frequency-dependent parameter $\kappa(\omega)$ should not be confused with the dc low-frequency dielectric constant $\kappa \equiv \varepsilon(0)/\varepsilon_0$ that was discussed in Chapter 3.

⁴⁷ As a reminder, the main properties of these functions are listed in Sec. 2.7 – see, in particular, Fig. 2.22 and Eqs. (2.157)-(2.158).

Finally, just as in the last section, we have to average the energy loss rate over random values of the impact parameter b :

$$-\frac{d\mathcal{E}}{dx} = \int \left(-\frac{d\mathcal{E}}{dV} \right) d^2b \approx 2\pi \int_{b_{\min}}^{\infty} \left(-\frac{d\mathcal{E}}{dV} \right) b db = 8\pi^2 \int_{b_{\min}}^{\infty} b db \int_0^{\infty} \left(|E_x|_{\omega}^2 + |E_y|_{\omega}^2 \right) \text{Im} \varepsilon(\omega) \omega d\omega. \quad (10.122)$$

Due to the (weak) divergence of the functions $K_0(\xi)$ and $K_1(\xi)$ at $\xi \rightarrow 0$, we have to cut the resulting integral over b at some b_{\min} where our theory loses legitimacy. (On that limit, we are not doing much better than in the past section). Plugging in the calculated expressions (116) and (117) for the field components, swapping the integrals over ω and b , and using the recurrence relations (2.142), which are valid for all Bessel functions, we finally get:

$$\boxed{-\frac{d\mathcal{E}}{dx} = \frac{2}{\pi} q^2 \text{Im} \int_0^{\infty} (\kappa^* b_{\min}) K_1(\kappa^* b_{\min}) K_0(\kappa^* b_{\min}) \frac{d\omega}{\omega \varepsilon(\omega)}}. \quad (10.123) \quad \text{Radiation intensity}$$

This general result is valid for a linear medium with arbitrary dispersion relations $\varepsilon(\omega)$ and $\mu(\omega)$. (The last function participates in Eq. (123) only via Eq. (115) that defines the parameter κ .) To get more concrete results, some particular model of the medium should be used. Let us explore the Lorentz-oscillator model that was discussed in Sec. 7.2, in its form (7.33) suitable for the transition to the quantum-mechanical description of atoms:

$$\varepsilon(\omega) = \varepsilon_0 + \frac{nq'^2}{m} \sum_j \frac{f_j}{(\omega_j^2 - \omega^2) - 2i\omega\delta_j}, \quad \text{with } \sum_j f_j = 1; \quad \mu(\omega) = \mu_0. \quad (10.124)$$

If the damping of the effective atomic oscillators is low, $\delta_j \ll \omega_j$, as it typically is, and the particle's speed u is much lower than the typical wave's phase velocity v (and hence than $c!$), then for most frequencies Eq. (115) gives

$$\kappa^2(\omega) \equiv \omega^2 \left[\frac{1}{u^2} - \frac{1}{v^2(\omega)} \right] \approx \frac{\omega^2}{u^2}, \quad (10.125)$$

i.e. $\kappa \approx \kappa^* \approx \omega/u$ is virtually real. In this case, Eq. (123) may be reduced to Eq. (95) with

$$b_{\max} = \frac{1.123u}{\langle \omega \rangle}. \quad (10.126)$$

The good news here is that both approaches (the microscopic analysis of Sec. 4 and the macroscopic analysis of this section) give essentially the same result. The same fact may be also perceived as bad news: the treatment of the medium as a continuum does not give any new results here. The situation somewhat changes at relativistic velocities, at which such treatment provides noticeable corrections (called *density effects*), in particular reducing the energy loss estimates.

Let me, however, leave these details for special topic courses and focus on a much more important effect described by our formulas. Consider the dependence of the electric field components on the impact parameter b , i.e. on the closest distance between the particle's trajectory and the field observation point. At $b \rightarrow \infty$, we can use, in Eqs. (116)-(117), the asymptotic formula (2.158),

$$K_n(\xi) \rightarrow \left(\frac{\pi}{2\xi} \right)^{1/2} e^{-\xi}, \quad \text{at } \xi \rightarrow \infty, \quad (10.127)$$

to conclude that if $\kappa^2 > 0$, i.e. if κ is real, the complex amplitudes E_ω of both components E_x and E_y of the electric field decrease with b exponentially. However, let us consider what happens at frequencies where $\kappa^2(\omega) < 0$,⁴⁸ i.e.

$$\varepsilon(\omega)\mu(\omega) \equiv \frac{1}{v^2(\omega)} < \frac{1}{u^2} < \frac{1}{c^2} \equiv \varepsilon_0\mu_0. \quad (10.128)$$

(This condition means that the particle's velocity is larger than the phase velocity of the waves at this particular frequency.) In this case, the parameter $\kappa(\omega)$ is purely imaginary, so the functions $\exp\{\kappa b\}$ in the asymptotes (127) of Eqs. (116)-(117) become just phase factors, and the field component amplitudes fall very slowly:

$$|E_x(\omega)| \propto |E_y(\omega)| \propto \frac{1}{b^{1/2}}. \quad (10.129)$$

This means that the Poynting vector drops as $1/b$, so its flux through a surface of a round cylinder of radius b , with its axis on the particle trajectory (i.e. the power flow from the particle), does not depend on b at all. This is an electromagnetic wave emission – the famous *Cherenkov radiation*.⁴⁹

The direction \mathbf{n} of its propagation may be readily found taking into account that at large distances from the particle's trajectory, the emitted wave has to be locally planar and transverse ($\mathbf{n} \perp \mathbf{E}$), so the so-called *Cherenkov angle* θ between the vector \mathbf{n} and the particle's velocity \mathbf{u} may be simply found from the ratio of the electric field components – see Fig. 14a:

$$\tan \theta = -\frac{E_x}{E_y}. \quad (10.130)$$

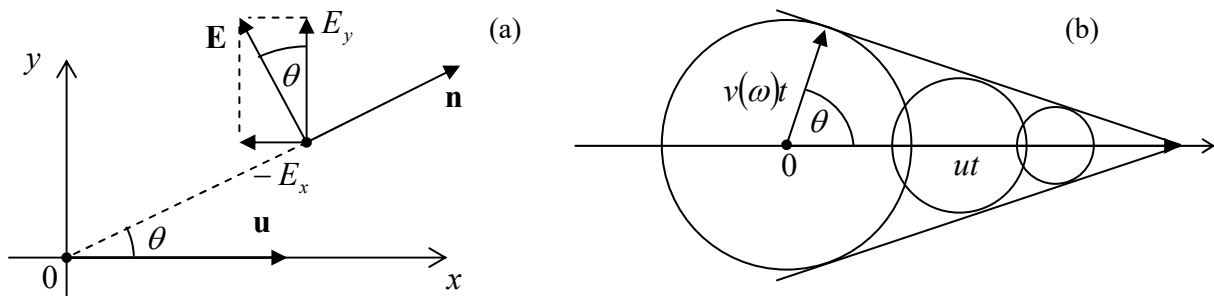


Fig. 10.14. (a) The Cherenkov radiation's propagation angle θ , and (b) its interpretation.

The ratio on the right-hand side of this relation may be calculated by plugging the asymptotic formula (127) into Eqs. (116) and (117) and calculating their ratio:

⁴⁸ Strictly speaking, the inequality $\kappa^2(\omega) < 0$ does not make sense for a medium with a complex product $\varepsilon(\omega)\mu(\omega)$, and hence complex $\kappa^2(\omega)$. However, in a typical medium where particles can propagate over substantial distances, the imaginary part of the product $\varepsilon(\omega)\mu(\omega)$ does not vanish only in very limited frequency intervals, much more narrow than the intervals that we are discussing now – please have one more look at Fig. 7.5.

⁴⁹ This radiation was observed experimentally by Pavel Alekseevich Cherenkov (in older Western texts, “Čerenkov”) in 1934, with the observations explained by Ilya Mikhailovich Frank and Igor Yevgenyevich Tamm in 1937. Note, however, that the effect had been predicted theoretically as early as 1889 by the same Oliver Heaviside whose name was mentioned in this course so many times – and whose genius I believe is still underappreciated.

$$\tan \theta = -\frac{E_x}{E_y} = \frac{i\kappa u}{\omega} = [\varepsilon(\omega)\mu(\omega)u^2 - 1]^{1/2} \equiv \left[\frac{u^2}{v^2(\omega)} - 1 \right]^{1/2}, \quad (10.131a)$$

so

$$\cos \theta = \frac{v(\omega)}{u} < 1. \quad (10.131b) \quad \text{Cherenkov radiation: angle}$$

Remarkably, this direction does not depend on the emission time t_{ret} , so the radiation of frequency ω , at each instant, forms a hollow cone led by the particle. This simple result allows an evident interpretation (Fig. 14b): the cone's interior is just the set of all observation points that have already been reached by the radiation, propagating with the speed $v(\omega) < u$, emitted from all previous points of the particle's trajectory by the given time t . This phenomenon is an analog of the so-called *Mach cone* in fluid dynamics,⁵⁰ besides that in the Cherenkov radiation, there is a separate cone for each frequency (of the range in which $v(\omega) < u$): the smaller is the $\varepsilon(\omega)\mu(\omega)$ product, i.e. the higher is the wave velocity $v(\omega) = 1/[\varepsilon(\omega)\mu(\omega)]^{1/2}$, the broader is the cone, so the earlier the corresponding "shock wave" arrives to an observer. Please note that the Cherenkov radiation is a unique radiative phenomenon: it takes place even if a particle moves without acceleration, and (in agreement with our analysis in Sec. 2), is impossible in free space, where $v(\omega) = c = \text{const}$ is larger than u for any particle.

The Cherenkov radiation's intensity may be also readily found by plugging the asymptotic expression (127), with imaginary κ , into Eq. (123). The result is

$$-\frac{d\mathcal{E}}{dx} \approx \left(\frac{\tilde{\varepsilon}e}{4\pi} \right)^2 \int_{v(\omega) < u} \omega \left[1 - \frac{v^2(\omega)}{u^2} \right] d\omega. \quad (10.132) \quad \text{Cherenkov radiation: intensity}$$

For non-relativistic particles ($u \ll c$), the Cherenkov radiation condition $u > v(\omega)$ is fulfilled only in relatively narrow frequency intervals where the product $\varepsilon(\omega)\mu(\omega)$ is very large (usually, due to optical resonance peaks of the electric permittivity – see Fig. 7.5 and its discussion). In this case, the emitted light consists of a few nearly-monochromatic components. On the contrary, if the condition $u > v(\omega)$, i.e. $u^2/\varepsilon(\omega)\mu(\omega) > 1$ is fulfilled in a broad frequency range, as it is for ultra-relativistic particles in condensed media, then the radiated power, according to Eq. (132), is dominated by higher frequencies of the range – hence the famous bluish color of the Cherenkov radiation glow from water-filled nuclear reactors– see Fig. 15.

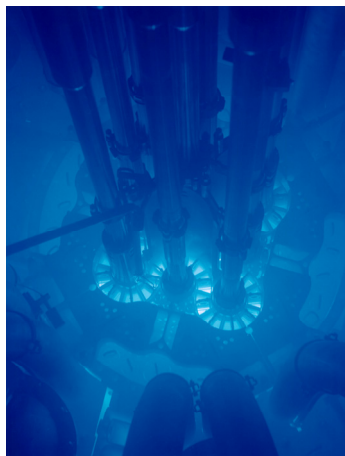


Fig. 10.15. The Cherenkov radiation glow in the Advanced Test Reactor of the Idaho National Laboratory in Arco, ID. (Adapted from http://en.wikipedia.org/wiki/Cherenkov_radiation under the Creative Commons CC-BY-SA-2.0 license.)

⁵⁰ Its brief discussion may be found in CM Sec. 8.6.

The Cherenkov radiation is broadly used in high-energy experiments for particle identification and speed measurement (since it is easy to pass the particles through layers of different densities and hence with different dielectric constants) – for example, in the so-called Ring Imaging Cherenkov (RICH) detectors that have been designed for the DELPHI experiment⁵¹ at the Large Electron-Positron Collider (LEP) in CERN.

A little bit counter-intuitively, the formalism described in this section is also very useful for the description of an apparently rather different effect – the so-called *transition radiation* that takes place when a charged particle crosses a border between two media.⁵² The effect may be interpreted as the result of the time dependence of the electric dipole formed by the moving charge q and its mirror image q' in the counterpart medium – see Fig. 16.

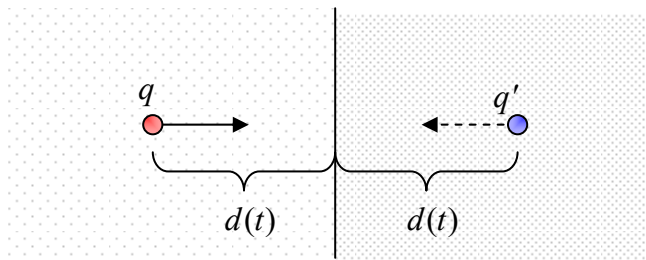


Fig. 10.16. The transition radiation's physics.

In the non-relativistic limit, this effect allows a straightforward description combining the electrostatics picture of Sec. 3.4 (see Fig. 3.9 and its discussion), and Eq. (8.27), corrected for the media polarization effects. However, if the particle's velocity u is comparable with the phase velocity of waves in either medium, the adequate theory of the transition radiation becomes very close to that of the Cherenkov radiation.

In comparison with the Cherenkov radiation, the transition radiation is rather weak, and its practical use (mostly for the measurement of the Lorentz factor γ , to which the radiation intensity is nearly proportional) requires multi-layered stacks.⁵³ In these systems, the radiation emitted at sequential borders may be coherent, and the system's physics may become close to that of the free-electron lasers mentioned in Sec. 4.

10.6. Radiation's back-action

An attentive and critically-minded reader could notice that so far our treatment of charged particle dynamics has never been fully self-consistent. Indeed, in Sec. 9.6 we have analyzed particle's motion in various external fields, ignoring those radiated by the particle itself, while in Sec. 8.2 and earlier in this chapter these fields have been calculated (admittedly, just for a few simple cases), but, again, their back-action on the emitting particle has been ignored. Only in very few cases we have taken

⁵¹ See, e.g., <http://delphiwww.cern.ch/offline/physics/delphi-detector.html>. For an in-depth review of radiation detectors (including the Cherenkov ones), the reader may be referred, for example, to the classical text by G. F. Knoll, *Radiation Detection and Measurement*, 4th ed., Wiley, 2010, and a newer treatment by K. Kleinknecht, *Detectors for Particle Radiation*, Cambridge U. Press, 1999.

⁵² The effect was predicted theoretically in 1946 by V. Ginzburg and I. Frank, and only later observed experimentally.

⁵³ See, e.g., Sec. 5.3 in K. Kleinknecht's monograph cited above.

the back effects of the radiation implicitly, via the energy conservation arguments. However, even in these cases, the near-field effects, such as the first term in Eq. (19), which affect the moving particle most, have been ignored.

At the same time, it is clear that in sharp contrast with electrostatics, the interaction of a moving point charge with its own field cannot be always ignored. As the simplest example, if an electron is made to fly through a resonant cavity, thus inducing electromagnetic oscillations in it, and then is forced (say, by an appropriate static field) to return into the cavity before the oscillations have decayed, its motion will certainly be affected by the oscillating fields, just as if they had been induced by another source. There is no conceptual problem with applying the Maxwell theory to such “field-particle rendezvous” effects; moreover, it is the basis of the engineering design of such vacuum electron devices as klystrons, magnetrons, and free-electron lasers.

A problem arises only when no clear “rendezvous” points are enforced by boundary conditions, so the most important self-field effects are at $R \equiv |\mathbf{r} - \mathbf{r}'| \rightarrow 0$, the most evident example being the charged particle’s radiation into free space, described earlier in this chapter. We already know that such radiation takes away a part of the charge’s kinetic energy, i.e. has to cause its deceleration. One should wonder, however, whether such self-action effects might be described in a more direct, non-perturbative way.

As the first attempt, let us try a phenomenological approach based on the already derived formulas for the radiation power \mathcal{P} . For the sake of simplicity, let us consider a non-relativistic point charge q in free space, so \mathcal{P} is described by Eq. (8.27), with the electric dipole moment’s derivative over time equal to $q\mathbf{u}$:

$$\mathcal{P} = \frac{Z_0 q^2}{6\pi c^2} \dot{\mathbf{u}}^2 \equiv \frac{2}{3c^3} \frac{q^2}{4\pi\epsilon_0} \dot{\mathbf{u}}^2. \quad (10.133)$$

The most naïve approach would be to write the equation of the particle’s motion in the form

$$m\dot{\mathbf{u}} = \mathbf{F}_{\text{ext}} + \mathbf{F}_{\text{self}}, \quad (10.134)$$

and try to calculate the radiation back-action force \mathbf{F}_{self} by requiring its instant power, $-\mathbf{F}_{\text{self}} \cdot \mathbf{u}$, to be equal to \mathcal{P} . However, this approach (say, for a 1D motion) would give a very unnatural result,

$$F_{\text{self}} \propto \frac{\dot{u}^2}{u}, \quad (10.135)$$

that might diverge at some points of the particle’s trajectory. This failure is clearly due to the retardation effect: as the reader may recall, Eq. (133) results from the analysis of radiation fields in the far-field zone, i.e. at *large* distances R from the particle, e.g., from the second term in Eq. (19), i.e. when the non-radiative first term (which is much larger at *small* distances, $R \rightarrow 0$) is ignored.

Before exploring the effects of this term, let us, however, make one more attempt at Eq. (133), considering its *average* effect on some periodic motion of the particle. (A possible argument for this step is that at the periodic motion, the retardation effects should be averaged out – just as at the transfer from Eq. (8.27) to Eq. (8.28).) To calculate the average, let us write the identity

$$\overline{\dot{\mathbf{u}}^2} \equiv \frac{1}{\mathcal{T}} \int_0^{\mathcal{T}} \dot{\mathbf{u}} \cdot \dot{\mathbf{u}} dt, \quad (10.136)$$

and carry out the integration on the right-hand side of Eq. (133) by parts over the motion period τ :

$$\overline{\mathcal{P}} = \frac{2}{3c^3} \frac{q^2}{4\pi\epsilon_0} \overline{(\dot{\mathbf{u}})^2} = \frac{2}{3c^3} \frac{q^2}{4\pi\epsilon_0} \frac{1}{\tau} \left(\dot{\mathbf{u}} \cdot \mathbf{u} \Big|_0^\tau - \int_0^\tau \ddot{\mathbf{u}} \cdot \mathbf{u} dt \right) = -\frac{1}{\tau} \int_0^\tau \frac{2}{3c^3} \frac{q^2}{4\pi\epsilon_0} \ddot{\mathbf{u}} \cdot \mathbf{u} dt. \quad (10.137)$$

On the other hand, the back-action force should give

$$\overline{\mathcal{P}} = -\frac{1}{\tau} \int_0^\tau \mathbf{F}_{\text{self}} \cdot \mathbf{u} dt. \quad (10.138)$$

These two averages coincide if⁵⁴

$$\mathbf{F}_{\text{self}} = \frac{2}{3c^3} \frac{q^2}{4\pi\epsilon_0} \ddot{\mathbf{u}}. \quad (10.139)$$

Abraham-
Lorentz
force

This is the so-called *Abraham-Lorentz force* of back-action. Before going after a more serious derivation of this formula, let us estimate its scale, representing Eq. (139) as

$$\mathbf{F}_{\text{self}} = m \tau \ddot{\mathbf{u}}, \quad \text{with } \tau \equiv \frac{2}{3mc^3} \frac{q^2}{4\pi\epsilon_0}, \quad (10.140)$$

where the constant τ evidently has the dimension of time. Recalling the definition (8.41) of the classical radius r_c of the particle, Eq. (140) for τ may be rewritten as

$$\tau = \frac{2}{3} \frac{r_c}{c}. \quad (10.141)$$

For the electron, τ is of the order of 10^{-23} s, so the right-hand side of Eq. (140) is very small. This means that in most cases the Abrahams-Lorentz force is either negligible or leads to the same results as the perturbative treatments of energy loss we have used earlier in this chapter.

However, Eq. (140) brings some unpleasant surprises. For example, let us consider a 1D oscillator with frequency ω_0 . For it, Eq. (134), with the back-action force given by Eq. (140), takes the form

$$m\ddot{x} + m\omega_0^2 x = m\tau \ddot{x}. \quad (10.142)$$

Looking for the solution of this linear differential equation in the usual exponential form, $x(t) \propto \exp\{\lambda t\}$, we get the following characteristic equation,

$$\lambda^2 + \omega_0^2 = \tau \lambda^3. \quad (10.143)$$

It may look like that for any “reasonable” value of $\omega_0 \ll 1/\tau \sim 10^{23} \text{ s}^{-1}$, the right-hand side of this nonlinear algebraic equation may be treated as a perturbation. Indeed, looking for its solutions in the

⁵⁴ Just for the reader’s reference, this formula may be readily generalized to the relativistic case, in the 4-form:

$$F_{\text{self}}^\alpha = \frac{2}{3mc^3} \frac{q^2}{4\pi\epsilon_0} \left[\frac{d^2 p^\alpha}{d\tau^2} + \frac{p^\alpha}{(mc)^2} \left(\frac{dp_\beta}{d\tau} \frac{dp^\beta}{d\tau} \right) \right],$$

– the so-called *Abraham-Lorentz-Dirac force*.

natural form $\lambda_{\pm} = \pm i\omega_0 + \lambda'$, with $|\lambda'| \ll \omega_0$, expanding both parts of Eq. (143) in the Taylor series in the small parameter λ' , and keeping only the terms linear in λ' , we get

$$\lambda' \approx -\frac{\omega_0^2 \tau}{2}. \quad (10.144)$$

This means that the energy of free oscillations decreases in time as $\exp\{2\lambda't\} = \exp\{-\omega_0^2 \tau t\}$; this is exactly the radiative damping analyzed earlier. However, Eq. (143) is deceiving; it has the third root corresponding to unphysical, exponentially growing (so-called *run-away*) solutions. It is easiest to see this for a free particle, with $\omega_0 = 0$. Then Eq. (143) becomes very simple,

$$\lambda^2 = \tau\lambda^3, \quad (10.145)$$

and it is easy to find all its three roots explicitly: $\lambda_1 = \lambda_2 = 0$ and $\lambda_3 = 1/\tau$. While the first two roots correspond to the values λ_{\pm} found earlier, the last one describes an exponential (and extremely rapid!) acceleration.

In order to remove this artifact, let us try to develop a self-consistent approach to the back-action effects, taking into account the near-field terms of particle fields. For that, we need to somehow overcome the divergence of Eqs. (10) and (19) at $R \rightarrow 0$. The most reasonable way to do this is to spread the particle's charge over a ball of radius a , with a spherically symmetric (but not necessarily constant) density $\rho(r)$, and at the end of the calculations trace the limit $a \rightarrow 0$.⁵⁵ Again sticking to the non-relativistic case (so the magnetic component of the Lorentz force is not important), we should calculate

$$\mathbf{F}_{\text{self}} = \int_V \rho(\mathbf{r}) \mathbf{E}(\mathbf{r}, t) d^3r, \quad (10.146)$$

where the electric field is that of the charge itself, with the field of any elementary charge $dq = \rho(r)d^3r$ described by Eq. (19).

To enable an analytical calculation of the force, we need to make the assumption $a \ll r_c$, treat the ratio $R/r_c \sim a/r_c$ as a small parameter, and expand the resulting right-hand side of Eq. (146) into the Taylor series in small R . This procedure yields

$$\mathbf{F}_{\text{self}} = -\frac{2}{3} \frac{1}{4\pi\epsilon_0} \sum_{n=0}^{\infty} \frac{(-1)^n}{c^{n+2} n!} \frac{d^{n+1} \mathbf{u}}{dt^{n+1}} \int_V d^3r \int_V d^3r' \rho(r) R^{n-1} \rho(r'). \quad (10.147)$$

The distance R cancels only in the term with $n = 1$,

$$\mathbf{F}_1 = \frac{2}{3c^3} \frac{\ddot{\mathbf{u}}}{4\pi\epsilon_0} \int_V d^3r \int_V d^3r' \rho(r) \rho(r') \equiv \frac{2}{3c^3} \frac{q^2}{4\pi\epsilon_0} \ddot{\mathbf{u}}, \quad (10.148)$$

showing that we have recovered (now in an *apparently* legitimate fashion) Eq. (139) for the Abrahams-Lorentz force. One could argue that in the limit $a \rightarrow 0$ the terms higher in $R \sim a$ (with $n > 1$) could be ignored. However, we have to notice that the main contribution to the series (147) is *not* described by Eq. (148) for $n = 1$, but is given by the much larger term with $n = 0$:

⁵⁵ Note: this operation cannot be interpreted as describing a quantum spread due to the finite extent of the point particle's wavefunction. In quantum mechanics, different parts of the wavefunction of the same charged particle do *not* interact with each other!

$$\mathbf{F}_0 = -\frac{2}{3} \frac{1}{4\pi\epsilon_0} \frac{\dot{\mathbf{u}}}{c^2} \int_V d^3r \int_V d^3r' \frac{\rho(r)\rho(r')}{R} \equiv -\frac{4}{3} \frac{\dot{\mathbf{u}}}{c^2} \frac{1}{4\pi\epsilon_0} \frac{1}{2} \int_V d^3r \int_V d^3r' \frac{\rho(r)\rho(r')}{R} \equiv -\frac{4}{3c^2} \dot{\mathbf{u}}U, \quad (10.149)$$

where U is the electrostatic energy (1.59) of the static charge's self-interaction. This term may be interpreted as the inertial "force"⁵⁶ ($-m_{\text{ef}}\mathbf{a}$) with the following effective *electromagnetic mass*:

$$m_{\text{ef}} = \frac{4}{3} \frac{U}{c^2}, \quad (10.150)$$

Electro-
magnetic
mass

which is a factor of 4/3 larger than it should be according to Einstein's formula (9.73). This is the famous (or rather infamous :-) *4/3 problem* that does not allow one to interpret the electron's mass as that of its electric field. Some (admittedly, rather formal) resolution of this paradox is possible only in quantum electrodynamics with its renormalization techniques – beyond the framework of this course.

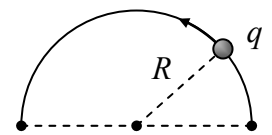
Note that all these issues are only important for motions with frequencies of the order of $1/\tau \sim 10^{23} \text{ s}^{-1}$, i.e. at energies as high as $\sim \hbar/\tau \sim 10^8 \text{ eV}$, while other quantum electrodynamics effects may be observed at much lower frequencies, starting from $\sim 10^{10} \text{ s}^{-1}$. Hence the 4/3 problem is by no means the only or the most significant motivation for the transfer from classical to quantum electrodynamics. However, the reader should not think that their time spent on this course has been lost: quantum electrodynamics is heavily based on classical electrodynamics, incorporates virtually all its results, and the basic transition between them is surprisingly straightforward.⁵⁷ So, I look forward to welcoming the reader to the next, quantum-mechanics part of this series.

10.6. Exercise problems

10.1. Derive Eqs. (10) from Eqs. (1) by a direct (but careful!) integration.

10.2. Derive the radiation-related parts of Eqs. (19)-(20) from the Liénard-Wiechert potentials (10) by direct differentiation.

10.3. A point charge q that was in a stationary position on a circle of radius R is carried over, along the circle, to the opposite position on the same diameter (see the figure on the right) as fast as only physically possible, and then is kept steady at this new position. Calculate and sketch the time dependence of its electric field \mathbf{E} at the center of the circle.



10.4. Express the instantaneous power of electromagnetic radiation by a relativistic particle with electric charge q and rest mass m , moving with velocity \mathbf{u} , via the Lorentz force \mathbf{F} providing its acceleration.

10.5. A relativistic particle with rest mass m and electric charge q , initially at rest, is accelerated by a constant force \mathbf{F} until it reaches a certain velocity u and then is left to move by inertia. Calculate the total energy radiated during the acceleration.

⁵⁶ See, e.g., CM Sec. 4.6.

⁵⁷ See, e.g., QM Secs. 9.1-9.4.

10.6. A charged relativistic particle with an initial momentum \mathbf{p}_0 flies ballistically from a free-space region into a region of a constant, uniform electric field \mathbf{E} , whose force is directed opposite to \mathbf{p}_0 . Calculate the energy radiated by the particle during its motion in the field, assuming that it is small in comparison with the particle's initial kinetic energy.

10.7. Calculate

- (i) the instantaneous power, and
- (ii)* the power spectrum

of the radiation emitted, into a unit solid angle, by a relativistic particle with charge q , performing 1D harmonic oscillations with frequency ω_0 and displacement amplitude a .

10.8. Calculate and analyze the time dependence of the energy of a charged relativistic particle rotating in a constant and uniform magnetic field \mathbf{B} and, as a result, emitting the synchrotron radiation. Qualitatively, what is the particle's trajectory?

Hint: You may assume that the energy loss is relatively slow ($-d\mathcal{E}/dt \ll \omega_e \mathcal{E}$), but should spell out the condition of validity of this assumption.

10.9. Analyze the polarization of the synchrotron radiation propagating within the particle's rotation plane.

10.10. Analyze the polarization and the spectral contents of the synchrotron radiation propagating in the direction normal to the particle's rotation plane. How do the results change if not one, but $N > 1$ similar particles move around the circle, at equal angular distances?

10.11.* The basic quantum theory of radiation shows that the electric dipole radiation by a particle is allowed only if the change of its angular momentum's magnitude L at the transition is of the order of Planck's constant \hbar .

- (i) Estimate the change of L of an ultra-relativistic particle due to its emission of a typical single photon of the synchrotron radiation.
- (ii) Do you think quantum mechanics forbid such radiation? If not, why?

10.12. A relativistic particle moves along the z -axis, with velocity u_z , through an undulator – a system of permanent magnets providing (in the simplest model) a perpendicular magnetic field, whose distribution near the axis is sinusoidal:⁵⁸

$$\mathbf{B} = \mathbf{n}_y B_0 \cos k_0 z .$$

Assuming that the field is so weak that it causes negligible deviations of the particle's trajectory from the straight line, calculate the angular distribution of the resulting radiation. What condition does the above assumption impose on the system's parameters?

⁵⁸ As the Maxwell equation for $\nabla \times \mathbf{H}$ shows, this field distribution cannot be created in any non-zero volume of free space. However, it may be created on a line – e.g., on the particle's trajectory.

10.13. Discuss possible effects of the interference of the undulator radiation from different periods of its static field distribution. In particular, calculate the angular positions of the power density maxima.

10.14. An electron launched directly toward a plane surface of a perfect conductor is instantly absorbed by it at the impact. Calculate the angular distribution and the frequency spectrum of the electromagnetic waves radiated at this event, provided that the initial kinetic energy T of the particle is much larger than the conductor's workfunction ψ .⁵⁹ Is your result valid near the conductor's surface?

10.15. A relativistic particle, with a rest mass m and an electric charge q , flies ballistically, with velocity u , by an immobile point charge q' , with an impact parameter b so large that the deviations of its trajectory from the straight line are negligible. Calculate the total energy loss due to the electromagnetic radiation during the passage. Quantify the conditions of validity of your result.

⁵⁹ See Sec. 2.9, in particular Fig. 2.27a.

**This page is
intentionally left
blank**